ESFR-SMART

Research and Innovation Action (RIA)

This project has received funding from the European Union's Horizon 2020 research and innovation programme under grant agreement No 754501.

Start date : 2017-09-01 Duration : 48 Months
http://esfr-smart-h2020.eu

Specification of the new core safety measures

Authors : Dr. Andrei RINEISKI (KIT), Clément Meriot (EDF), Christine Coquelet (CEA), Jiri Krepel (PSI), Emil Fridman (HZDR), Konstantin Mikityuk (PSI)

ESFR-SMART - Contract Number: 754501
European Sodium Fast Reactor Safety Measures Assessment and Research Tools Roger Garbil

Document title	Specification of the new core safety measures
Author(s)	Dr. Andrei RINEISKI, Clément Meriot (EDF), Christine Coquelet (CEA), Jiri Krepel (PSI), Emil Fridman (HZDR), Konstantin Mikityuk (PSI)
Number of pages	45
Document type	Deliverable
Work Package	WP01
Document number	D1.2
Issued by	KIT
Date of completion	2018-07-19 09:47:08
Dissemination level	Public

Summary

The ESFR-SMART core description has been established in several steps on the basis of ESFR-EH core design proposed for the EURATOM CP-ESFR project and experiences gained in EURATOM ESNII+ project. In CP-ESFR core optimization studies aimed at Na void effect reduction, it was proposed ? following earlier studies worldwide ? to modify the axial part about the fissile region in order include the Na plenum and absorber region above. Also the lower steel reflector was replaced by the lower fertile blanket for the same reason. Introduction of corium discharge tubes was proposed in CP-ESFR as they may facilitate molten fuel discharge and exclude recriticalities after fuel melting. The ESFR-SMART optimizations studies are based on the CP-ESFR and ESNII+ ones. The axial arrangement above the core (Na plenum and absorber) of CP-ESFR was adopted. For further Na void effect reduction, it was proposed to reduce the inner core fissile height: following late CP-ESFR and ESNII+ studies. Unlike ESNII+, an option was considered to keep the upper fissile boundaries at similar axial locations in the inner and outer cores. The ESFR-SMART core includes extra fuel subassemblies at the outer core periphery in order to compensate the inner fissile height reduction. It was also aimed to use the same fuel enrichments in the inner and outer cores, if possible. The corium discharge tubes were included: at the central position, between inner and outer cores, and at the core periphery. The number of DSD locations, including those for passive safety devices, was increased. The axial part between the fissile region and lower gas plenum was proposed to be a combination of the fertile lower blanket and steel reflector below: to reduce the sodium void effect, but prevent breeding. The fissile and fertile heights and single fissile enrichment were finally chosen on the basis of fine optimization studies. A 6-batch fuel reloading scheme was proposed, instead of a 5-batch one in CP-ESFR. The core is surrounded by 2 rings of steel reflector and 1 ring of absorber subassemblies. Outside of absorber there are locations for spent fuel subassemblies, including 3 inner and 3 outer core batches. In the new ESFRSMART core, the calculated void effect is significantly reduced: to a value well below 1$ at the end of cycle. In the following, core specifications are given, which can be most easily used for deterministic neutronics codes such as ERANOS. These specifications contain dimensions and nuclear...

Approval

Date	By
2018-07-19 10:20:28	Mr. Enrico GIRARDI (EDF)
2018-07-19 11:25:43	Dr. Konstantin MIKITYUK (PSI)

European Commission

Horizon 2020
European Union funding
for Research & Innovation

Action	Research and Innovation Action NFRP-2016-2017-1
Grant Agreement #	754501
Project name	European Sodium Fast Reactor Safety Measures Assessment and Research Tools
Project Acronym	ESFR-SMART
Project start date	01.09.2017
Deliverable #	D1.1.2.
Title	Specification of the new core safety measures
Author(s)	A. Rineiski (KIT); C. Mériot (EDF); C. Coquelet-Pascal (CEA); J. Krepel (PSI), E. Fridman (HZDR), K. Mikityuk (PSI)
Version	11
Related WP	WP1.1. New safety measures
Related Task	T1.1.2. Specification of the new core safety measures (KIT)
Lead organization	KIT
Submission date	01.05.2018
Dissemination level	CO

This project has received funding from the Euratom research and training programme 2014-2018 under the grant agreement n°754501

History

Date	Submitted by	Reviewed by	Version (Notes)
18.01.2018	C. Meriot (EDF)		01
24.01.2018		K. Mikityuk (PSI)	02
26.01.2018		C. Meriot (EDF)	03: Absorber above the plenum changed to B4C with natural B
12.03.2018		A. Rineiski (KIT)	04: Summary added. Appendix added: core description for Monte-Carlo codes prepared by E. Fridman (HZDR)
22.03.2018		A. Rineiski (KIT)	05: Nuclear densities for the fuel with 17.317 wt% enrichment in Table 3, Appendix to be updated
24.03.2018		K. Mikityuk (PSI)	06: 1) The report is re-organized to integrate Appendix in the report body 2) Table 12. "Radial layout: CSD" Pin pitch changed from 4.3150 cm to 2.4300 cm, number of pins from 19 to 37 and materials from "B4C Nat" to "B4C Nat / B4C Enriched" 3) A mistake fixed on Fig.1 (at one position i5 is replaced by i6) 4) Table "Absorber characteristics" removed, because it is not consistent with Tables 12 and 13.
24.03.2018		A. Carascosa (UPM)	07: Table 10 "Radial layout: Fertile fuel" Pellet material changed from MOX tu UOX
29.03.2018		E. Fridman (HZDR)	07: 1) Table 19 is removed 2) Table 20 is updated for the fuel with 17.317 wt% enrichment (Table 19 in current version)
13.04.2018		E. Fridman (HZDR)	08: 1) Table 3 is updated 2) Table 18 and 19 are updated (new MOX/UOX densities and compositions)
14.04.2018		K. Mikityuk (PSI)	09: 1) K. Mikityuk is added to the list of co-authors 2) The paragraph about PCSS is added above Fig. 2 3) Fig. 2 corrected to make the design of the hydraulic rod equivalent to the design of DSD 4) The explanation is added to first bullet of Section 2.3: "The cladding volume and outer dimension were increased to account for the smearing effect: compare outer clad radius in Table 9 (0.5358 cm) and in Table 2 (0.5335 cm)."
14.04.2018		B. Lindley (WOOD)	09: The legend of inner and outer fuel on Fig. 1 chenged
23.04.2018		C. Meriot (EDF)	10: The Appendix is added which is EDF report "Core design optimization with the SDDS multi-physics and multi-objective method"
23.04.2018		K. Mikityuk (PSI)	10: The paragraph to summary added which shortly describes the added appendix. Table Of Content added.
01.05.2018		K. Mikityuk (PSI)	11: The paragraph added to Section 2.5 to explain that the number density corresponds to the real density and geometry of the fissile fuel pellet.

Table of Contents

1. Summary

The ESFR-SMART core description has been established in several steps on the basis of ESFR-EH core design proposed for the EURATOM CP-ESFR project and experiences gained in EURATOM ESNII+ project. In CP-ESFR core optimization studies aimed at Na void effect reduction, it was proposed – following earlier studies worldwide – to modify the axial part about the fissile region in order include the Na plenum and absorber region above. Also the lower steel reflector was replaced by the lower fertile blanket for the same reason. Introduction of corium discharge tubes was proposed in CP-ESFR as they may facilitate molten fuel discharge and exclude re-criticalities after fuel melting.

The ESFR-SMART optimizations studies are based on the CP-ESFR and ESNII+ ones. The axial arrangement above the core (Na plenum and absorber) of CP-ESFR was adopted. For further Na void effect reduction, it was proposed to reduce the inner core fissile height: following late CP-ESFR and ESNII+ studies. Unlike ESNII+, an option was considered to keep the upper fissile boundaries at similar axial locations in the inner and outer cores. The ESFR-SMART core includes extra fuel subassemblies at the outer core periphery in order to compensate the inner fissile height reduction. It was also aimed to use the same fuel enrichments in the inner and outer cores, if possible. The corium discharge tubes were included: at the central position, between inner and outer cores, and at the core periphery. The number of DSD locations, including those for passive safety devices, was increased. The axial part between the fissile region and lower gas plenum was proposed to be a combination of the fertile lower blanket and steel reflector below: to reduce the sodium void effect, but prevent breeding. The fissile and fertile heights and single fissile enrichment were finally chosen on the basis of fine optimization studies. A 6-batch fuel reloading scheme was proposed, instead of a 5-batch one in CP-ESFR.

The core is surrounded by 2 rings of steel reflector and 1 ring of absorber subassemblies. Outside of absorber there are locations for spent fuel subassemblies, including 3 inner and 3 outer core batches. In the new ESFR-SMART core, the calculated void effect is significantly reduced: to a value well below 1$ at the end of cycle.

In the following, core specifications are given, which can be most easily used for deterministic neutronics codes such as ERANOS. These specifications contain dimensions and nuclear densities at the room temperature, temperatures related to operating conditions, and tables for thermal expansion. To facilitate model preparations and calculations with Monte-Carlo codes, an additional dataset for a simplified core description at operating conditions is also provided.

The appendix contains the EDF report on details of the core design optimization with the SDDS multi-physics and multi-objective method.

2. Core specification

2.1 Nominal conditions

The ESFR-SMART core is a modification of the ESFR-WH core, proposed by CEA for the FP7 CP-ESFR project. The initial ESFR-WH core description is given in [1], modifications are given in [2]. The current document describes the version proposed in WP1.1 of the ESFR-SMART project in January 2018. The nominal conditions of the ESFR-SMART reactor are listed in Table 1.

Table 1. Nominal conditions

Parameter	Value
Reactor power (MWth)	3600
Core inlet temperature (°C)	395
Core outlet temperature (°C)	545
Average sodium temperature (°C)	470
Average core structure temperature (°C)	470
Average fuel temperature (°C)	1227
Average fertile materials temperature (°C)	627

2.2 Radial core map

Figure 1 shows the ESFR-SMART core layout in plane. In total there are 216 Inner core subassemblies (S/As), 288 Outer core S/As, 31 Corium discharge tubes, 24 CSD S/As, 12 DSD S/As, 66 R1 (First reflector ring) S/As, 96 R2 (Second reflector ring) S/As and, 102 R3 (Third reflector ring) S/As.

It is assumed that the irradiated inner core S/As are stored in the hexagonal ring next to the Third reflector ring. The irradiated outer core S/As are stored in the following rings as shown in Figure 1.

The number of positions for spent fuels S/A has to be defined from the total number of fuel S/A (216 inner S/A and 288 outer S/A, for a total of 504 S/A). The size is optimized to deal with 3 batches to store (corresponding to 252 S/A.

The core is finally composed of 13 rings of fuel S/A, 3 rings of reflector then 2 rings of spent fuel internal storage positions and 4 rings of shielding. Assuming the hexagonal S/A pitch being equal to 21 cm, the minimum barrel diameter reaches 8.8 m.

A reloading scheme with 6 batches is proposed by PSI (Figure 1). Neutronics characteristics (reactivity, void effect, breeding gain, power map, control rods efficiency, *etc.*) have to be evaluated for the initial core but also for the equilibrium core by taking into account the reloading of fuel batches.

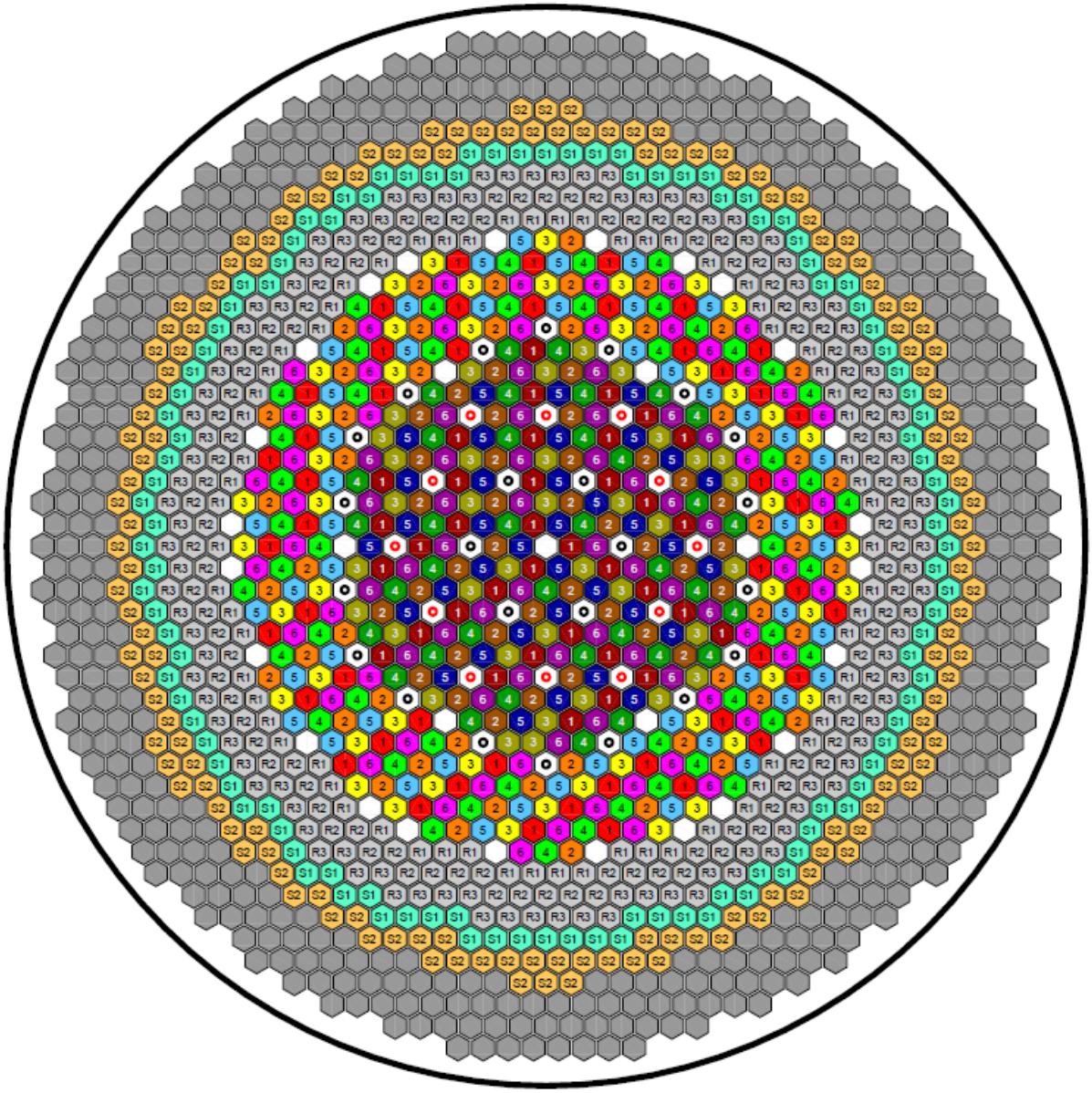

Figure 1. Radial layout of the mixed reloading schemes for the ESFR-SMART core.

1 2 3 4 5 6	Inner fuel	6 batches×36 = 216
1 2 3 4 5 6	Outer fuel	6 batches×48 = 288
○ ○	CSD / DSD	24 / 12
R1 R2 R3	1st / 2nd /3rd reflector ring	66 / 96 / 102
S1	Spent Inner / Outer fuel storage	3 batches×36 = 108
S2	Spent Inner / Outer fuel storage	3 batches×48 = 144
	Corium discharge tubes	31

2.3 Radial layout of subassemblies

As fabricated fuel S/A geometry is shown in Table 2.

Table 2. As fabricated fuel S/A geometry

S/A Pitch (cm)	20.985
Sodium gap width (mm)	4.5
Wrapper tube outer width (cm)	20.535
Wrapper tube thickness (mm)	4.5
Spacer wire diameter (cm)	0.1
Number of fuel pins per S/A	271
Outer clad radius (cm)	0.5335
Clad thickness (cm)	0.05

The following should be noted:

- The spacer wires were not explicitly modelled but were smeared with the cladding. The cladding volume and outer dimension were increased to account for the smearing effect: compare outer clad radius in Table 9 (0.5358 cm) and in Table 2 (0.5335 cm).
- The radial reflectors R1 and R2 have the same radial geometry and composition as axial reflector in fuel assemblies.
- The radial reflector R3 has the same radial geometry and composition as axial absorber in fuel assemblies.
- Sodium plenum and follower are modelled as sodium inside subassembly wrapper (i.e. no pin lattice structure).
- Head and foot are modelled as homogeneous mixtures (Table 20) inside subassembly wrapper (i.e. no pin lattice structure).

The fuel S/A dimensions provided in Table 2 correspond to the “as fabricated” conditions (i.e. 20°C). The actual neutronics calculations are expected to be performed assuming nominal operating conditions (Table 3). The thermal expansions in the neutronics analysis are accounted for using the following assumptions:

- Sub-assembly pitch is expanded using a single global radial expansion coefficient given in Table 3. This coefficient is derived from linear expansion data of EM10. The global radial expansion is driven by the inlet Na temperature.
- All axial dimensions are expanded using a single global axial expansion coefficient given in Table 3. This coefficient is derived from linear expansion data of EM10. Global axial expansion is driven by core-average Na temperature.
- Radial dimensions of individual pins, cladding, wrappers, etc. are expanded using corresponding expansion coefficient shown in Table 3.
- The material densities are decreased to preserve the total mass

A detailed description of the “as fabricated” and nominal dimensions and material compositions are provided in the following sections.

Table 3. Nominal temperatures and corresponding thermal expansion coefficients

Material	Nominal operating conditions*		
	T(°C) for thermal expansion	Expansion coefficient	T(K) for ACE files
MOX fissile	1227	1.0139	1500
MOX fertile	627	1.0065	900
ODS	470	1.0056	900
EM10	470	1.0054	900
B4C	627	1.0029	900
Na	470	1.0431	900
Global radial (EM10)	395	1.0044	-
Global axial (EM10)	470	1.0054	-

* "As fabricated" conditions: T(°C) = 20; T(K) = 300

Table 4. Radial layout: Sub-assembly wrapper

		Nominal T, °C	ACE file T, K
Material for global radial expansion	EM10	395	
Wrapper material	EM10	470	900
	Cold dim.	Rad. expn. coeff.	Nominal dim.
S/A pitch flat-to-flat (cm)	20.9850	*1.0044*	21.07797
Wrapper inner flat-to-flat/2 (cm)	9.8175	*1.0054*	9.87051
Wrapper outer flat-to-flat/2 (cm)	10.2675	*1.0054*	10.32294

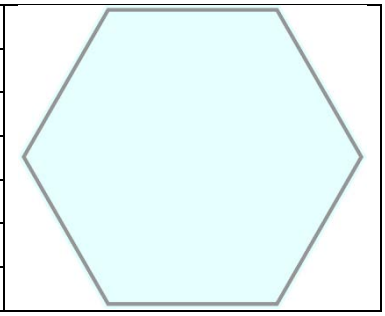

Table 5. Radial layout: Axial and Radial reflector (R1 and R2)

Axial reflector / Radial reflector R1 and R2			
Number of pins	19	Rad. expn. coeff.	Nominal dim.
Pin pitch (cm)	4.3150		
		Nominal T, °C	ACE file T, K
Pellet material	EM10	470	900
Gap material	EM10	470	900
Cladding material	EM10	470	900
	Cold dim.	Rad. expn. coeff.	Nominal dim.
Pellet radius (cm)	1.9000	*1.0054*	1.91032
Clad inner radius (cm)	1.9000	*1.0054*	1.91032
Clad outer radius (cm)	2.0062	*1.0054*	2.01709

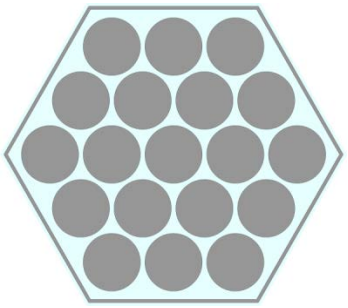

Table 6. Radial layout: Axial absorber and Radial reflector (R3)

Axial Absorber / Radial reflector R3			
Number of pins	19	Rad. expn. coeff.	Nominal dim.
Pin pitch (cm)	4.3150		
		Nominal T, °C	ACE file T, K
Pellet material	B4C Nat	627	900
Gap material	He	470	900
Cladding material	EM10	470	900
	Cold dim.	Rad. expn. coeff.	Nominal dim.
Pellet radius (cm)	1.8000	*1.0029*	1.80520
Clad inner radius (cm)	1.9000	*1.0054*	1.91032
Clad outer radius (cm)	2.0062	*1.0054*	2.01709

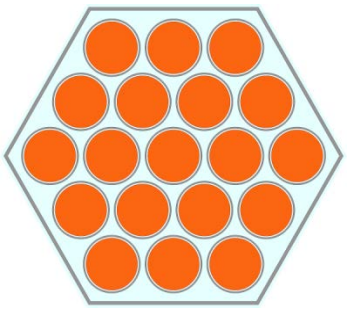

Table 7. Radial layout: Upper/Lower plug

Upper/Lower plug			
Number of pins	271	Rad. expn. coeff.	Nominal dim.
Pin pitch (cm)	1.1670		
		Nominal T, °C	ACE file T, K
Pellet material	ODS	470	900
Gap material	ODS	470	900
Cladding material	ODS	470	900
	Cold dim.	Rad. expn. coeff.	Nominal dim.
Pellet radius (cm)	0.4835	*1.0056*	0.48623
Clad inner radius (cm)	0.4835	*1.0056*	0.48623
Clad outer radius (cm)	0.5358	*1.0056*	0.53886

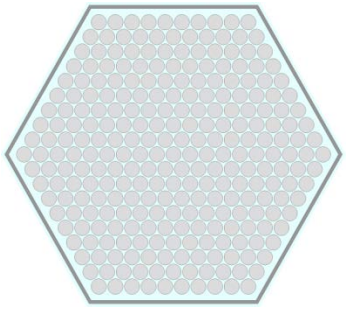

Table 8. Radial layout: Upper/Lower gas plenum

Upper/Lower gas plenum			
Number of pins	271	Rad. expn. coeff.	Nominal dim.
Pin pitch (cm)	1.1670		
		Nominal T, °C	ACE file T, K
Plenum material	He	470	900
Cladding material	ODS	470	900
	Cold dim.	Rad. expn. coeff.	Nominal dim.
Clad inner radius (cm)	0.4835	*1.0056*	0.48623
Clad outer radius (cm)	0.5358	*1.0056*	0.53886

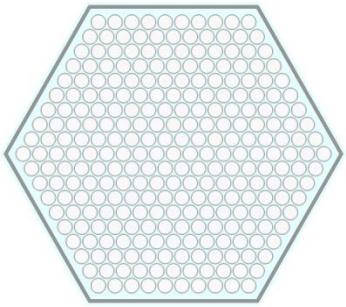

Table 9. Radial layout: Fissile fuel

Fuel fissile			
Number of pins	271	Rad. expn. coeff.	Nominal dim.
pin pitch (cm)	1.1670		
		Nominal T, °C	ACE file T, K
Pellet material	MOX	1227	1500
Gap material	He	470	900
Cladding material	ODS	470	900
	Cold dim.	Rad. expn. coeff.	Nominal dim.
Pellet inner hole radius (cm)	0.1560	*1.0139*	0.15816
Pellet radius (cm)	0.4680	*1.0139*	0.47448
Clad inner radius (cm)	0.4835	*1.0056*	0.48623
Clad outer radius (cm)	0.5358	*1.0056*	0.53886

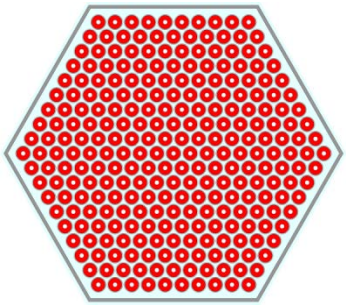

Table 10. Radial layout: Fertile fuel

Fuel fertile				
Number of pins	271	Rad. expn. coeff.	Nominal dim.	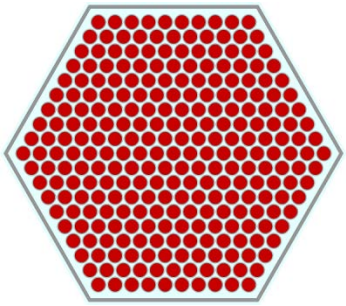
Pin pitch (cm)	1.1670			
		Nominal T, °C	ACE file T, K	
Pellet material	UOX	627	900	
Gap material	He	470	900	
Cladding material	ODS	470	900	
	Cold dim.	Rad. expn. coeff.	Nominal dim.	
Pellet radius (cm)	0.4680	*1.0065*	0.47105	
Clad inner radius (cm)	0.4835	*1.0056*	0.48623	
Clad outer radius (cm)	0.5358	*1.0056*	0.53886	

Table 11. Radial layout: Lower steel blanket

Lower steel blanket				
Number of pins	271	Rad. expn. coeff.	Nominal dim.	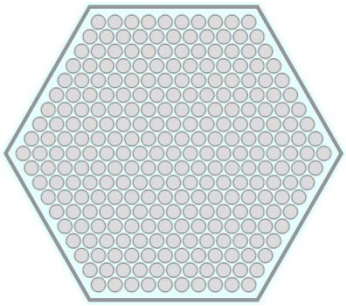
Pin pitch (cm)	1.1670			
		Nominal T, °C	ACE file T, K	
Pellet material	ODS	470	900	
Gap material	He	470	900	
Cladding material	ODS	470	900	
	Cold dim.	Rad. expn. coeff.	Nominal dim.	
Pellet radius (cm)	0.4680	*1.0056*	0.47064	
Clad inner radius (cm)	0.4835	*1.0056*	0.48623	
Clad outer radius (cm)	0.5358	*1.0056*	0.53886	

Table 12. Radial layout: CSD

CSD				
Number of pins	37	Rad. expn. coeff.	Nominal dim.	
Pin pitch (cm)	2.4300			
		Nominal T, °C	ACE file T, K	
Pellet material	B4C Nat B4C Enriched	627	900	
Gap material	He	470	900	
Cladding material	EM10	470	900	
Internal wrapper material	EM10	470	900	
	Cold dim.	Rad. expn. coeff.	Nominal dim.	
Pellet radius (cm)	0.9150	*1.0029*	0.91764	
Clad inner radius (cm)	1.0415	*1.0054*	1.04716	
Clad outer radius (cm)	1.1412	*1.0054*	1.14741	
Internal wrapper inner flat-to-flat/2 (cm)	7.6000	*1.0054*	7.64129	
Internal wrapper outer flat-to-flat/2 (cm)	7.8000	*1.0054*	7.84238	

Table 13. Radial layout: DSD

DSD				
Number of pins	55	Rad. expn. coeff.	Nominal dim.	
Pin pitch (cm)	1.7420			
		Nominal T, °C	ACE file T, K	
Pellet material	B4C Nat or B4C Enriched	627	900	
Gap material	He	470	900	
Cladding material	EM10	470	900	
Internal wrapper material	EM10	470	900	
	Cold dim.	Rad. expan. coeff.	Nominal dim.	
Pellet radius (cm)	0.7000	*1.0029*	0.70202	
Clad inner radius (cm)	0.7665	*1.0054*	0.77066	
Clad outer radius (cm)	0.8189	*1.0054*	0.82339	
Internal wrapper inner flat-to-flat/2 (cm)	7.2000	*1.0054*	7.23912	
Internal wrapper outer flat-to-flat/2 (cm)	7.4000	*1.0054*	7.44020	

2.4 Axial core map

Compared to the ESFR-WH core, the following major modifications are done in the axial layout in order to reduce reactivity effects in case of sodium boiling under hypothetical accident conditions (see Figure 2 and Figure 3):

- a large sodium plenum topped by absorber is introduced above the core;
- the inner and outer core heights are reduced by 250 and 50 mm, respectively (1000 mm in ESFR-WH core), and
- a lower fertile blanket is introduced below the fuel, with a steel blanket below (with axial dimensions in mm).

The enrichment is the same in the inner and outer core zones. The fertile pellet has the same radius as the fuel, but no inner hole and a different isotopic composition: the Pu enrichment is zero. The composition of depleted uranium and plutonium (data from the CP-ESFR project) used for fresh fuel is specified in Table 19. A near-zero Pu balance was targeted while performing core optimization. The steel compositions (ODS for fuel clad and EM10 for hexagonal tube, (data from CP-ESFR project) are detailed in Table 20. The Plenum is similar to Follower, i.e. sodium insider wrapper, but with different Na temperatures/densities. Information on CSD, DSD, lower gas plenum (LGP), upper gas plenum (UGP), lower axial blanket (LAB), plug is available in [1, 2]. Information on ABS, REFL, Fertile is given below.

In ESFR-SMART there are 31 corium discharge tubes which were not included in the ESFR-WH. The geometry is the same as in the sodium plenum below the Na plenum upper axial boundary. Above this boundary: the same as in fuel SAs at the corresponding height. i.e. absorber and UCS. For reminder, the Na plenum / corium discharge tube is composed of a hexagonal tube and sodium.

Passive Core Shutdown Systems (PCSS) are considered as follows:

- In the reference core all 12 DSD rods are of Curie Point Electro Magnet (CPEM) type.
- A sensitivity study for selected transients will be performed in Task 1.3.4 for an alternative core in which all DSD rods will be hydraulic rods, i.e. triggered by reduction of the flowrate.

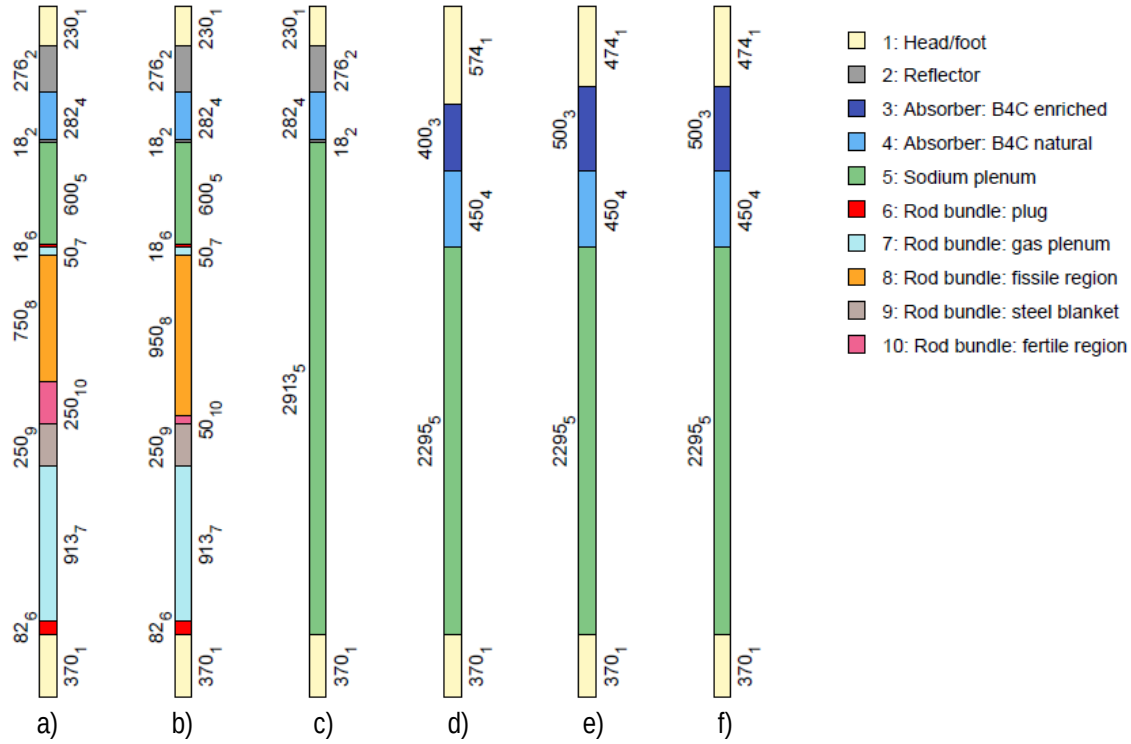

Figure 2. Axial composition of ESFR-SMART core subassemblies (length in mm and subscripts indicate the material ID): a) inner fuel; b) outer fuel; c) corium discharge tube; d) CSD; e) DSD; f) hydraulic control rod.

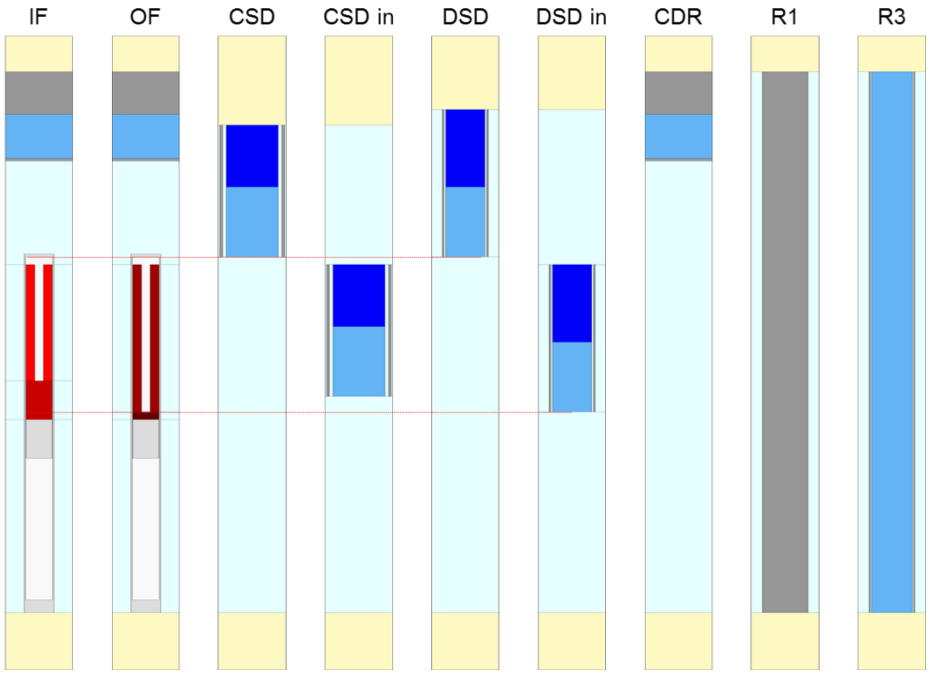

Figure 3. Axial layouts of the ESFR-SMART core sub-assemblies with indication of the homogeneous and heterogeneous regions

The axial dimensions are provided for all ESFR-SMART core sub-assemblies including inner fuel (IF) and outer fuel (OF) (Table 14), CSD and DSD (Table 15), corium discharge rod (CDR) (Table 16), and radial reflector (RR) (Table 17). Note that at the parking position, the bottom of the control rod is aligned with the top of the upper gas plenum and not with the top of the active core (Figure 3).

Table 14. Axial dimensions: inner and outer fuel

		IF				OF			
		Region height (cm)		Cumulative height (cm)		Region height (cm)		Cumulative height (cm)	
#	Axial region	cold	nominal	cold	nominal	cold	nominal	cold	nominal
1	Foot	37.000	37.201	0.000	0.000	37.000	37.201	0.000	0.000
2	Lower plug	8.200	8.245	37.000	37.201	8.200	8.245	37.000	37.201
3	Lower gas plenum	91.300	91.796	45.200	45.446	91.300	91.796	45.200	45.446
4	Lower steel blanket	25.000	25.136	136.500	137.242	25.000	25.136	136.500	137.242
5	Fertile	25.000	25.136	161.500	162.377	5.000	5.027	161.500	162.377
6	Fissile	75.000	75.407	186.500	187.513	95.000	95.516	166.500	167.405
7	Upper gas plenum	5.000	5.027	261.500	262.921	5.000	5.027	261.500	262.921
8	Upper plug	1.800	1.810	266.500	267.948	1.800	1.810	266.500	267.948
9	Na plenum	60.000	60.326	268.300	269.758	60.000	60.326	268.300	269.758
10	Reflector	1.800	1.810	328.300	330.084	1.800	1.810	328.300	330.084
11	Absorber	28.200	28.353	330.100	331.893	28.200	28.353	330.100	331.893
12	Reflector	27.600	27.750	358.300	360.247	27.600	27.750	358.300	360.247
13	Head	23.000	23.125	385.900	387.996	23.000	23.125	385.900	387.996
	sum	408.900	411.121	408.900	411.121	408.900	411.121	408.900	411.121

Table 15. Axial dimensions: CSD and DSD

		CSD				DSD			
		Region height (cm)		Cumulative height (cm)		Region height (cm)		Cumulative height (cm)	
#	Axial region	cold	nominal	cold	nominal	cold	nominal	cold	nominal
1	Foot	37.00	37.201	0.000	0.000	37.00	37.201	0.000	0.000
2	Na plenum	229.50	230.747	37.000	37.201	229.50	230.747	37.000	37.201
3	B4C nat.	45.00	45.244	266.500	267.948	45.00	45.244	266.500	267.948
4	B4C enrch.	40.00	40.217	311.500	313.192	50.00	50.272	311.500	313.192
5	Head	57.40	57.712	351.500	353.410	47.40	47.658	361.500	363.464
	sum	408.900	411.121	408.900	411.121	408.900	411.121	408.900	411.121

Table 16. Axial dimensions: Corium discharge tube

	Cor. Disch	Region height (cm)		Cumulative height (cm)	
#	Axial region	cold	nominal	cold	nominal
1	Foot	37.000	37.201	0.000	0.000
2	Na plenum	291.300	292.883	37.000	37.201
3	Reflector	1.800	1.810	328.300	330.084
4	Absorber	28.200	28.353	330.100	331.893
5	Reflector	27.600	27.750	358.300	360.247
6	Head	23.000	23.125	385.900	387.996
	sum	408.900	411.121	408.900	411.121

Table 17. Axial dimensions: Radial reflector

	RR	Region height (cm)		Cumulative height (cm)	
#	Axial region	cold	nominal	cold	nominal
1	Foot	37.000	37.201	0.000	0.000
2	Reflector	348.900	350.795	37.000	37.201
3	Head	23.000	23.125	385.900	387.996
	sum	408.900	411.121	408.900	411.121

2.5 Isotopic compositions of core materials

Note that the number densities given in Table 19 correspond to the real physical density of the fuel and to the real fissile fuel pellet geometry with the inner hole, but not to the “smeared” density and geometry.

Table 18. Fuel characteristics

Fuel residence time (EFPD)	2170
Fuel Burnup (GWd/t)	100
Inner fissile fuel enrichment (%wt)	17.99
Outer fissile fuel enrichment (%wt)	17.99
Fissile fuel average density	10.542 (95.5% TD)
Fertile fuel average density	10.457 (95.5% TD)

Table 19. Isotopic composition of fresh fissile and fertile fuel (“as fabricated” and nominal operating conditions)

Fissile	T, °C	20 °C	1227 °C
Nuclide	ID	ND, 1/b·cm	ND, 1/b·cm
O-16	8016	4.65494E-02	4.50318E-02
U-235	92235	4.88798E-05	4.72863E-05
U-238	92238	1.92567E-02	1.86289E-02
Pu-238	94238	1.51237E-04	1.46306E-04
Pu-239	94239	1.99840E-03	1.93325E-03
Pu-240	94240	1.24561E-03	1.20500E-03
Pu-241	94241	3.44245E-04	3.33022E-04
Pu-242	94242	4.32159E-04	4.18070E-04
Am-241	95241	3.25801E-05	3.15180E-05
Total	Total	7.00592E-02	6.77752E-02

Fertile	T, °C	20 °C	627 °C
Nuclide	ID	ND, 1/b·cm	ND, 1/b·cm
O-16	8016	4.66425E-02	4.57818E-02
U-235	92235	5.98785E-05	5.87736E-05
U-238	92238	2.32622E-02	2.28329E-02
Total		6.99646E-02	6.86735E-02

Table 20. Steel compositions (weight fractions)

Elements	ODS (MA956)	
Density (20°C)	7.25 g/cm^3	
Fe	70.08	Fe54 : 5.8
		Fe56 : 91.72
		Fe57 : 2.2
		Fe58 : 0.28
Cr	21.5	Cr50 : 4.34
		Cr52 : 83.81
		Cr53 : 9.49
		Cr54 : 2.36
Al	5.75	Al : 100
Y_2O_3	0.7	Y_2O_3 : 100
Ti	0.6	Ti : 100
Ni	0.5	Ni : 100
Mn	0.3	Mn : 100
Co	0.3	Co : 100
Cu	0.15	Cu : 100
C	0.1	C : 100
P	0.02	P : 100

Elements	EM10	
Density (20°C)	7.76 g/cm^3	
Fe	89	Fe54 : 5.8
		Fe56 : 91.72
		Fe57 : 2.2
		Fe58 : 0.28
Cr	8.5	Cr50 : 4.34
		Cr52 : 83.81
		Cr53 : 9.49
		Cr54 : 2.36
Ni	0.5	Ni58 : 68.27
		Ni60 : 26.1
		Ni61 : 1 13
		Ni62 : 3.59
		Ni64 : 0.91
Mo	1	Mo : 100
Mn	0.5	Mn : 100
C	0.1	C : 100
Ti+Nb+W	0.02	Ti : 100
Si	0.3	Si : 100

Table 21. Isotopic composition of ODS and EM10 (“as fabricated” and nominal operating conditions)

ODS	T, °C	20 °C	470 °C
Nuclide	ID	ND, 1/b·cm	ND, 1/b·cm
Fe-54	26054	3.29005E-03	3.23502E-03
Fe-56	26056	5.01723E-02	4.93331E-02
Fe-57	26057	1.18229E-03	1.16251E-03
Fe-58	26058	1.47881E-04	1.45408E-04
Cr-50	24050	8.15672E-04	8.02029E-04
Cr-52	24052	1.51468E-02	1.48935E-02
Cr-53	24053	1.68269E-03	1.65454E-03
Cr-54	24054	4.10708E-04	4.03838E-04
Al-27	13027	9.30443E-03	9.14880E-03
O-16	8016	4.05824E-04	3.99036E-04
Y-89	39089	2.70750E-04	2.66221E-04
Ti-46	22046	4.70308E-05	4.62441E-05
Ti-47	22047	4.15112E-05	4.08168E-05
Ti-48	22048	4.02768E-04	3.96031E-04
Ti-49	22049	2.89537E-05	2.84693E-05
Ti-50	22050	2.71694E-05	2.67149E-05
Ni-58	28058	2.57242E-04	2.52939E-04
Ni-60	28060	9.50713E-05	9.34810E-05
Ni-61	28061	4.04852E-06	3.98080E-06
Ni-62	28062	1.26551E-05	1.24434E-05
Ni-64	28064	3.10748E-06	3.05550E-06
Mn-55	25055	2.38417E-04	2.34429E-04
Co-59	27059	2.22254E-04	2.18537E-04
Cu-63	29063	7.19643E-05	7.07606E-05
Cu-65	29065	3.11175E-05	3.05970E-05
C-12	6012	3.63838E-04	3.57752E-04
P-31	15031	2.81919E-05	2.77203E-05
Total		8.46962E-02	8.32795E-02

EM10	T, °C	20 °C	470 °C
Nuclide	ID	ND, 1/b·cm	ND, 1/b·cm
Fe-54	26054	4.47222E-03	4.39921E-03
Fe-56	26056	6.81999E-02	6.70866E-02
Fe-57	26057	1.60710E-03	1.58086E-03
Fe-58	26058	2.01017E-04	1.97735E-04
Cr-50	24050	3.45160E-04	3.39525E-04
Cr-52	24052	6.40952E-03	6.30489E-03
Cr-53	24053	7.12045E-04	7.00421E-04
Cr-54	24054	1.73795E-04	1.70958E-04
Ni-58	28058	2.75338E-04	2.70843E-04
Ni-60	28060	1.01759E-04	1.00098E-04
Ni-61	28061	4.33331E-06	4.26257E-06
Ni-62	28062	1.35453E-05	1.33242E-05
Ni-64	28064	3.32607E-06	3.27178E-06
Mo-92	42092	7.51009E-05	7.38750E-05
Mo-94	42094	4.59330E-05	4.51832E-05
Mo-95	42095	7.82918E-05	7.70138E-05
Mo-96	42096	8.12772E-05	7.99504E-05
Mo-97	42097	4.61020E-05	4.53494E-05
Mo-98	42098	1.15463E-04	1.13578E-04
Mo-100	42100	4.52315E-05	4.44931E-05
Mn-55	25055	4.25314E-04	4.18371E-04
C-12	6012	3.89432E-04	3.83075E-04
Ti-46	22046	1.67797E-06	1.65058E-06
Ti-47	22047	1.48104E-06	1.45687E-06
Ti-48	22048	1.43700E-05	1.41355E-05
Ti-49	22049	1.03301E-06	1.01615E-06
Ti-50	22050	9.69353E-07	9.53529E-07
Si-28	14028	4.62133E-04	4.54589E-04
Si-29	14029	2.26672E-05	2.22971E-05
Si-30	14030	1.44495E-05	1.42136E-05
Total		8.43400E-02	8.29632E-02

Table 22. Isotopic composition of natural and 90% enriched B_4C ("as fabricated" and nominal operating conditions)

B4C Nat.	T, °C	20 °C	627 °C
Nuclide	ID	ND, 1/ b·cm	ND, 1/ b·cm
B-10	5010	2.26535E-02	2.23969E-02
B-11	5011	8.29305E-02	8.19913E-02
C	6012	2.63960E-02	2.60971E-02
Total		1.31980E-01	1.30485E-01

B4C 90%	T, °C	20 °C	627 °C
Nuclide	ID	ND, 1/ b·cm	ND, 1/ b·cm
B-10	5010	9.57424E-02	9.46581E-02
B-11	5011	9.67525E-03	9.56567E-03
C	6012	2.63544E-02	2.60559E-02
Total		1.31772E-01	1.30280E-01

Table 23. Sodium at different temperatures

Sodium	T, °C	20 °C	470 °C	545 °C
Nuclide	ID	ND, 1/ b·cm	ND, 1/ b·cm	ND, 1/ b·cm
Na-23	11023	2.48851E-02	2.19235E-02	2.14078E-02

Table 24. Homogeneous mixtures (volume fractions)

	Na	EM10
Head	81.5%	18.5%
Foot	76.5%	23.5%

3. References

1. D. Blanchet. L. Buiron. 2008. "ESFR. Working Horses. Core concept definition". FP-7-ESFR. Technical Report. CEA.

2. D. Struwe. 2010. "Core datafile.xls". Additional specifications distributed after the Bologna meeting. June 2010.

4. Appendix A. Core design optimization with the SDDS multi-physics and multi-objective method

EDF R&D

PERFORMANCE ET PREVENTION DES RISQUES INDUSTRIELS DU PARC PAR LA SIMULATION ET LES ETUDES

SURETE ET PHYSIQUE DU CYCLE

7 boulevard Gaspard Monge 91120 PALAISEAU - +33 (1) 78 19 32 00

17/04/2018

ESFR-SMART T1.1.2: Core design optimization with the SDDS multi-physics and multi-objective method

Clement MERIOT

EDF R&D - PERICLES

6125-1109-2018-00387-FR	1.0		
Type d'information : Note technique			

Following the previous FP7 European project CP-ESFR, a new project called ESFR-SMART started in September 2017. It considers the Generation-IV safety objectives and the state-of-the-art European and international safety frameworks. This report corresponds to the work performed by EDF for Task 1.1.2 of the ESFR-SMART project.

A preliminary core design was proposed by KIT ans PSI, improving the previous ESFR-CONF2 axial layout. The present study aims for a more precise optimization of the fuel sub-assemblies (S/As) axial structure and of the fuel pins geometry, in order to improve the void effect and reach a near-zero breeding-gain, while keeping the cycle length higher than 2000 EFPD (Equivalent Full Power Day). The SDDS multi-physic tool has been used to evaluate the performances of a large number of core designs and select the most optimized ones, in agreement with the constraints of the project. It permitted to reduce the void effect below 0.5$ at end of equilibrium cycle (reduction by 80% with respect to the initial design), reach an average breeding gain of -0.5%, and simplify the sub-assembly geometry. The selected design has been validated with the ESFR-SMART partners.

Circuit de validation

Auteur	Clement MERIOT	12/04/2018	
Vérificateur	Sandra POUMEROULY	13/04/2018	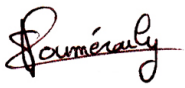
Approbateur	Enrico GIRARDI	17/04/2018	

Code affaire	**P11G5**

 © EDF SA 2018

Liste de diffusion

Groupe destinataire
11-PERICLES Chefs groupe
11-PERICLES Chefs
11-PERICLES Antenne gestion

Pré-diff	Diff	Destinataire	Structure	E-mail
	X	AMICE Laurent	EDF R&D - DIR R&D	laurent.amice@edf.fr
	X	ANDRIOLO Lena	EDF R&D - PERICLES	lena.andriolo@edf.fr
	X	BEILS Stéphane	FRAMATOME	stephane.beils@framatome.com
	X	BITTAN Jeremy	EDF R&D - PERICLES	jeremy.bittan@edf.fr
	X	BORE Clement	EDF R&D - MFEE	clement.bore@edf.fr
	X	BUBELIS Evaldas	KIT	evaldas.bubelis@kit.edu
	X	COQUELET Christine	CEA	christine.coquelet@cea.fr
	X	DELMAERE Thomas	EDF R&D - MFEE	thomas.delmaere@edf.fr
	X	FRIDMAN Emil	HZDR	e.fridman@hzdr.de
	X	GICQUEL Solene	EDF R&D - MMC	solene.gicquel@edf.fr
X	X	GIRARDI Enrico	EDF R&D - PERICLES	enrico.girardi@edf.fr
	X	KREPEL Jiri	PSI	jiri.krepel@psi.ch
X	X	LAVAUD Franck	EDF R&D - PERICLES	franck.lavaud@edf.fr
	X	LEMASSON David	EDF R&D - PERICLES	david.lemasson@edf.fr
	X	MARCHETTI Marco	KIT	marco.marchetti@kit.edu
	X	MASSARA Simone	EDF R&D - PERICLES	simone.massara@edf.fr
	X	MERIOT Clement	EDF R&D - PERICLES	clement.meriot@edf.fr
	X	MIKITYUK Konstantin	PSI	konstantin.mikityuk@psi.ch
	X	PONOMAREV Alexander	PSI	alexander.ponomarev@psi.ch
X	X	POUMEROULY Sandra	EDF R&D - PERICLES	sandra.poumerouly@edf.fr
	X	RINEISKI Andrei	KIT	andrei.rineiski@kit.edu
	X	SCHMITT Damien	EDF R&D - PERICLES	damien.schmitt@edf.fr

 © EDF SA 2018

AVERTISSEMENT / CAUTION

L’accès à ce document, ainsi que son utilisation, sont strictement limités aux personnes expressément habilitées par EDF.

EDF ne pourra être tenu responsable, au titre d'une action en responsabilité contractuelle, en responsabilité délictuelle ou de toute autre action, de tout dommage direct ou indirect, ou de quelque nature qu'il soit, ou de tout préjudice, notamment, de nature financière ou commerciale, résultant de l'utilisation d'une quelconque information contenue dans ce document.

Les données et informations contenues dans ce document sont fournies "en l'état" sans aucune garantie expresse ou tacite de quelque nature que ce soit.

Toute modification, reproduction, extraction d’éléments, réutilisation de tout ou partie de ce document sans autorisation préalable écrite d’EDF ainsi que toute diffusion externe à EDF du présent document ou des informations qu’il contient est strictement interdite sous peine de sanctions.

The access to this document and its use are strictly limited to the persons expressly authorized to do so by EDF.

EDF shall not be deemed liable as a consequence of any action, for any direct or indirect damage, including, among others, commercial or financial loss arising from the use of any information contained in this document.

This document and the information contained therein are provided "as are" without any warranty of any kind, either expressed or implied.

Any total or partial modification, reproduction, new use, distribution or extraction of elements of this document or its content, without the express and prior written consent of EDF is strictly forbidden. Failure to comply to the above provisions will expose to sanctions.

Executive Summary

This report corresponds to the work performed by EDF for Task 1.1.2 of the ESFR-SMART European project.

Following the previous FP7 European project CP-ESFR, a new project called ESFR-SMART started in September 2017. It considers the Generation-IV safety objectives and the state-of-the-art European and international safety frameworks.

This study is part of the task T1.1.2 “Specification of the new core safety measures” involving KIT, PSI, CEA and EDF, in the Work Package 1.1 “New Safety Measures”.

A first core design was proposed by KIT, improving the previous ESFR-CONF2 axial layout. A radial layout was drawn with the partners, and PSI provided a 6-batches reloading scheme. The present study aims for a more precise optimization of the fuel sub-assemblies (S/As) axial structure and of the fuel pins geometry.

This optimization has two main objectives, which are to improve the void effect and reach a near-zero breeding-gain, while keeping the cycle length higher than 2000 EFPD (Equivalent Full Power Day). Secondary goals were chosen, in agreement with the constraints of the project: the reduction of the core diameter, a unique Pu enrichment in the core, or the simplification of the axial structure of the sub-assembly by pooling the heights of the fuel or fertile parts.

A two-steps procedure has been followed, as in previous studies: after a first pass of optimization with the SDDS methodology, we use the surrogate models to create an optimized design of experiment, focused on the interesting area of the performances space. We simulate and krige again this new design of experiments to build better quality surrogate models and reduce the prediction uncertainty.

A final core design was chosen and validated with the ESFR-SMART partners. Compared to the initial design, it has a reduced pin radius and an increased fuel pellet hole radius, a unique Pu content, an increased fertile blanket height and a reduced fuel height. It permitted to reduce the void effect below 0.5$ at end of equilibrium cycle, reach a breeding gain of 0.5% in mean, and simplify the sub-assembly and therefore the further studies.

Summary

1. Introduction

Following the previous FP7 European project CP-ESFR, a new project called ESFR-SMART started in September 2017. This project considers the Generation-IV safety objectives and the state-of-the-art European and international safety standards.

This study is part of the task T1.1.2 “Specification of the new core safety measures” involving KIT, PSI, CEA and EDF, within the Work Package 1.1 “New Safety Measures”.

A first core design was proposed by KIT, improving the previous ESFR-CONF2 axial layout. A radial layout was drawn with the partners, and PSI provided a 6-batches reloading scheme. The present study aims for a more precise optimization of the fuel sub-assemblies (S/As) axial and internal structures, by using a multi-physics and multi-objective optimization tool called SDDS.

First, the general method SDDS, developed at EDF, will be explained. Then, the study of the initial design and the optimization process will be detailed. The selected core design is specified at the end of the document.

2. Method overview

The global objective of the SDDS method is to help the designer by giving him a first simplified overall perspective. The tool has three aims:

- Provide a multi-physics analysis. Neutronics, thermal-hydraulics transients and thermal-mechanics can be dealt with simultaneously, in order to try to catch a global optimum.
- Ensure an exhaustive scan of the available design options. The whole parameters space is swept, so that no interesting configuration is let aside.
- Build a physical data base. Once the calculations have been performed, the selection of a design is made very quickly. If the objectives or the set of requirements of the design are changed within a certain range, no additional calculation is needed.

The general layout of the method is given in Fig.1.

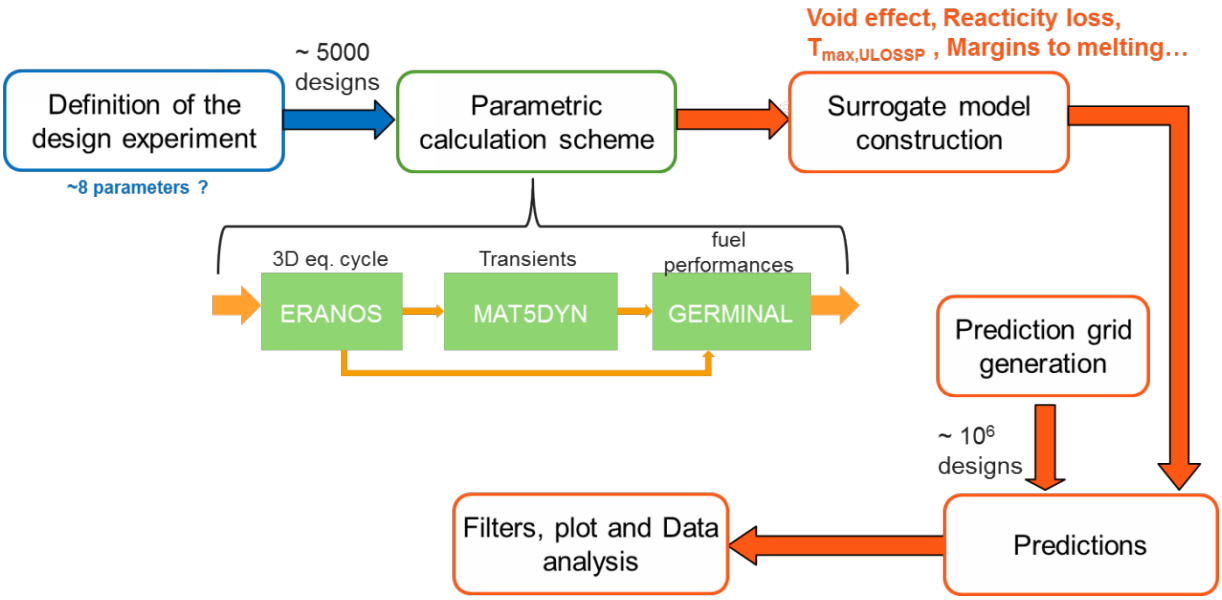

Fig. 1 – General layout of the SDDS method

First, a design of experiment has to be defined: the designer has to choose the number of parameters, their range of variation, and the distribution of the core designs (see §3.2), which must be wisely chosen

so as to sweep the whole design space. The quality of the design of experiment is optimized by an entropy-maximization method [1], using the DiceDesign R package [2].

Then, the performances of this set of core designs are evaluated with a multi-physics calculation scheme, using ERANOS [3], MAT5DYN [4] and GERMINAL [5] for 3D-neutronics, multichannel transient and fuel performances analysis, respectively. The neutronics calculation scheme set up with ERANOS is composed of the following steps, to evaluate the performances of each design and feed the further transient and thermal-mechanics calculations:

- First, we adjust the plutonium content in the inner and outer cores for each design to ensure criticality at End Of Cycle (EOC) plus a reactivity margin set to 700 pcm and minimize the maximal sub-assembly power over the core. These calculations are performed with a neutron transport code in 3D geometry (VARIANT solver), with inserted control rods and following the mentioned fuel reloading scheme to achieve equilibrium. The 33-group cross-sections for neutron transport calculations are prepared with a cell module of ERANOS with a fine scheme for active zones (heterogeneous geometry, library with 1968 energy groups).
- The fuel depletion simulations until equilibrium and study of equilibrium cycle are performed.
- The feedback calculation uses a diffusion solver in 3D geometry except for sodium void worth and sodium expansion effect which are calculated with a transport code in 2D RZ geometry.
- Finally, a complete set of data for Unprotected Control Rod Withdrawal (UCRW) calculations is established using a neutron transport code in 3D geometry. The reactivity worth and power shape swing induced by each individual rod removal are evaluated.

MAT5DYN uses a multi-channel description, a simplified pin thermal evaluation, and a point kinetics neutronics model to simulate several transients: Unprotected Loss Of Flow (ULOF), Unprotected Loss of Heat Sink (ULOHS), Unprotected Loss of Service Station Power (ULOSSP), and Unprotected Transient Over Power (UTOP, simulated in order to determine relative elevations of core power due to reactivity insertions during UCRW transients). It uses a single-phase description of the coolant, and an extrapolation of the coolant temperature after reaching the boiling temperature. As we only perform comparative analyses, this approximation is suitable.

Fuel pin thermal-mechanics calculations are performed with GERMINAL. The maximum linear power is taken from neutronics calculations. For each core configuration and for each cycle of its equilibrium campaign, the hottest sub-assemblies are simulated to determine the minimal margin to fuel melting at nominal conditions, and for each control rod withdrawal, the hottest fuel sub-assemblies are simulated to determine their linear power leading to fuel melting. The safety margin during UCRW is then evaluated as the difference between the linear power leading to fuel melting and the maximum linear heat rate at the end of the UCRW, considering the relative elevation of power calculated with MAT5DYN and uncertainties to ensure the non-melting with 95% confidence. More details about the calculation scheme are given in [6].

We create a data basis containing the physical data related to each core configuration in nominal and accidental conditions. This data basis is used as an input for an interpolation method. The one used in SDDS is kriging (also called Gaussian Process Regression) [7]. This method performs an unbiased interpolation which is suitable for deterministic codes. This process allows to generate a set of meta-models (or surrogate, one per performance) that can be used instead of the calculation codes in order to “predict” quickly the performances of any core design. Each meta-model is validated using an independent set of calculations. Moreover, Kriging provides a confidence interval for the prediction of the surrogate model, which is very helpful to remove the non-physical points, with a leave-one-out method.

Then, the performances of a very large amount of core designs are quickly predicted (~10^6 designs).

3. Optimization study

3.1. Initial core design

The nominal conditions of the reactor are listed in table 1.

Parameter	Value
Reactor power (MWth)	3600
Core inlet temperature (°C)	395
Core outlet temperature (°C)	545
Average core structure temperature (°C)	470
Average fuel temperature (°C)	1227
Average fertile materials temperature (°C)	627

Table 1 – Nominal conditions of the ESFR-SMART reactor

The radial and axial layout of the initial core was proposed by KIT (see minutes of the T1.1.2 meeting on 24th October 2017), based on the CP-ESFR core design [8] with some modifications. Fig. 2 presents the radial layout with 216 inner fuel (yellow), 288 outer fuel (red), 24 CSD (grey), 12 DSD (dark grey), 31 discharge tubes (purple) and at least 3 rows of reflector S/As (white). A 6-batch 120° symmetric reloading scheme was developed by PSI (Fig.4).

 © EDF SA 2018

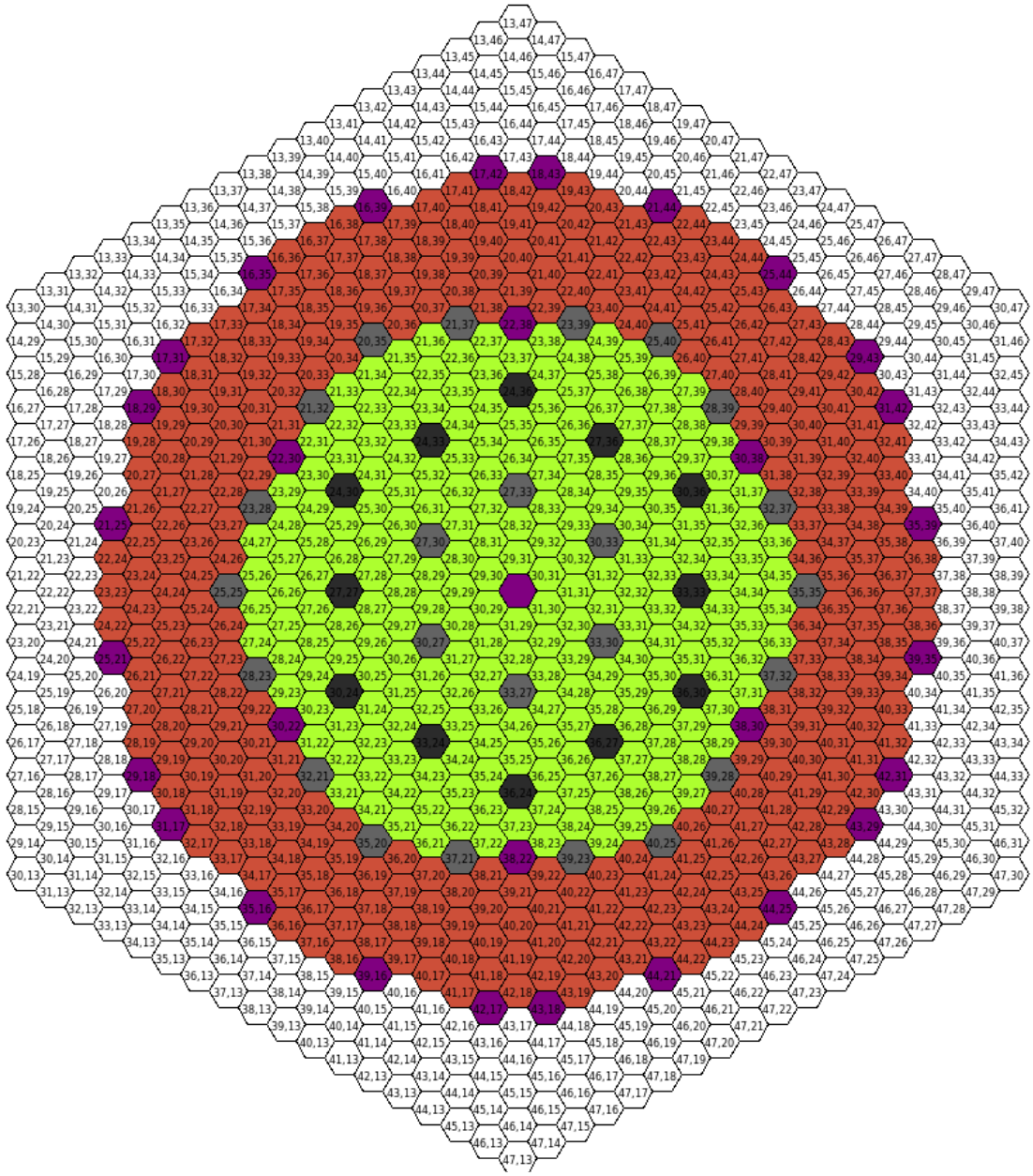

Fig. 2 – Radial layout of the ESFR-SMART core (KIT,CEA,PSI)

The axial layout proposed by KIT is given on Fig.3. Compared to the ESFR core, two major modifications are done in the axial layout in order to reduce reactivity effects in case of sodium boiling under hypothetical accident conditions: a large sodium plenum is introduced above the active core, and a steel blanket is added below the fertile blanket.

An identical Pu enrichment is used in the inner/outer fuel S/As. The fuel characteristics are listed in table 2.

Fig. 3 – Axial layout of the initial core design

Target Fuel residence time (EFPD)	>2000
Target Discharged Fuel Burnup (GWd/t)	100
Inner fuel enrichment (%wt)	17
Outer fuel enrichment (%wt)	17
S/A Pitch (cm)	21.08
Sodium gap width (mm)	4.5
Wrapper tube outer width (cm)	20.63
Wrapper tube thickness (mm)	4.5
Spacer wire diameter (cm)	0.1
Number of fuel pins per S/A	271
Outer clad radius (cm)	0.5365
Clad thickness (cm)	0.05
Cladding material	ODS
Fuel pellet radius (cm)	0.4865
Fuel pellet's inner hole radius (cm)	0.125
Fertile pellet radius (cm)	0.4865
Fuel average density	95.5% TD

Table 2 – Fuel characteristics of the initial core design : M2 configuration (KIT)

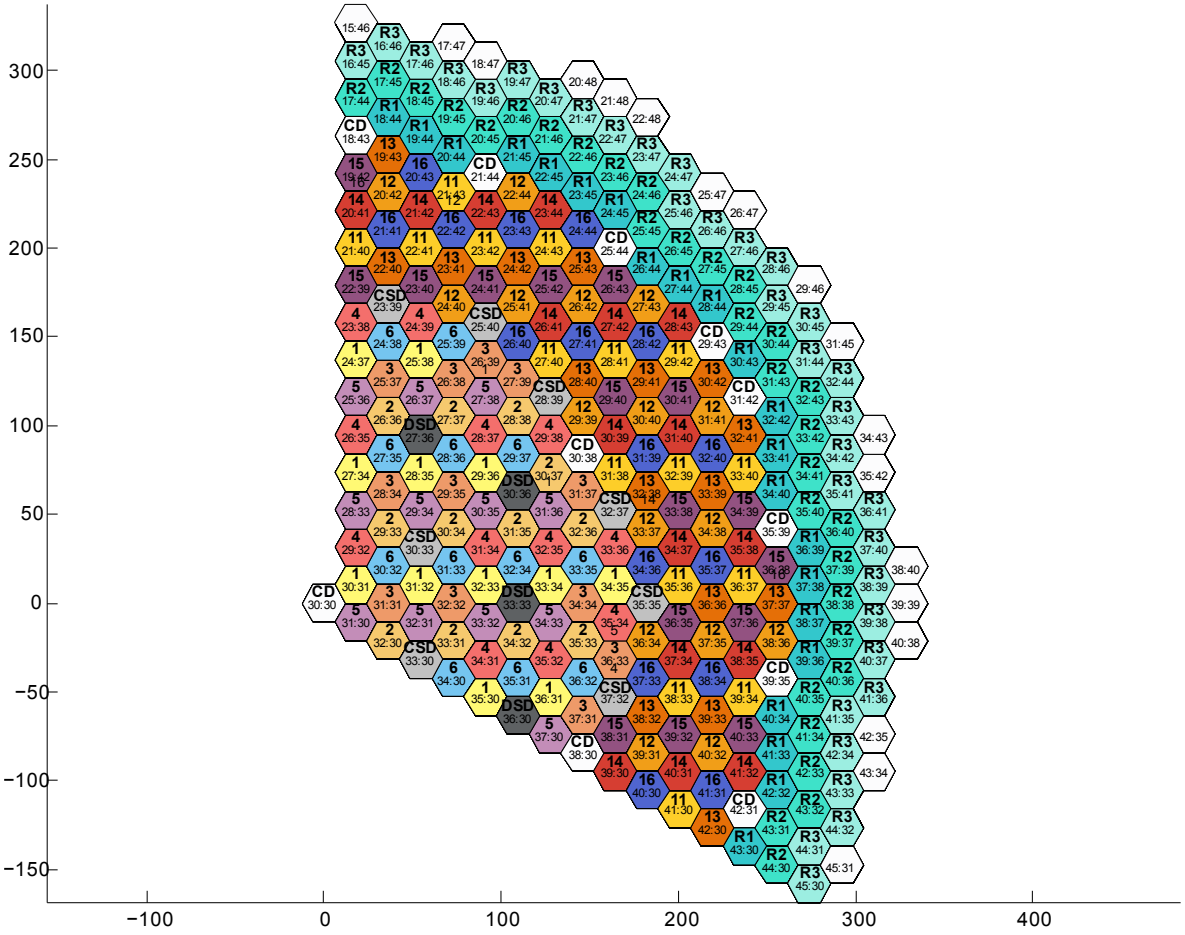

Fig. 4 - Reloading scheme used for the whole study (PSI)

Some performances of this initial core design (called M2) were evaluated during the Equilibrium Cycle with the multi-physics calculation scheme used in SDDS (Table 3). The Extended Sodium Void Effect (SVRE, including active core + UGP + plug + sodium plenum void effects) at End Of Equilibrium Cycle (EOEC) is higher than 2$ ($=368pcm), and the mean breeding gain is slightly low, but the behaviour of the core during an Unprotected Control Rod Withdrawal (UCRW) is quite satisfying.

The main objectives of the further optimization are to reduce the SVRE, to slightly increase the breeding gain, and to improve the ULOSSP and UCRW behaviour as much as possible. A reduction of the core diameter would be appreciated.

	Initial (M2)
Inner Enrich. (%wt)	17
Outer Enrich. (%wt)	17
Cycle length (EFPD)	**2195**
Breeding Gain	**-5.2%**
Total SVRE (pcm) at EOEC	**765**
Estimated max. Na T°C in ULOSSP (°C)	*1000**
Minimal Margin to melting in UCRW (W/cm)	11
KD fiss+fert (°C) 1227 --> 2300 °C	-886

Table 3 – Performances of the initial core design

*Obtained with a monophasic calculation code. The sodium temperature is extrapolated after reaching the ebullition temperature. This value is an approximation.

3.2. Design of experiment

The radial layout and the reloading scheme are kept identical for whole optimization study: they are the same for each core of the design of experiment.

8 parameters have been modified (table 4):

- A fertile plate of variable **height** and **position** has been added (see Fig.5) in the inner fuel assembly. Increasing the fertile plate height (F) reduces the inner steel blanket's height in order to maintain a reasonable fissile fuel height;
- An Inner/Outer (D) **offset with a variable height** is added at the top of the active core;
- The **outer core height** (H);
- The **pellet radius** and the **inner clad radius**;
- The **spacer wire diameter**;
- The **number of pins** per fuel S/A;

Some constraints have been added:

- As the increase of the fuel pellet's inner hole radius is a win-win parameter for both ULOSSP and UCRW behaviour, we maintain it equal to 1/3 of the pellet's radius;
- As some parameters (dimension of the pins, number of pins per S/A) have an impact on the calculation of the S/A pitch and thus the core diameter, we limit the increase of the active core diameter to +10% of the initial core diameter of 5.5m.

 © EDF SA 2018

Fig. 5 - Axial structure's parameters for the optimization study

	Actual (M2 layout)	Min	Max
Pellet radius (cm)	0.4715	0.3	0.5
Cladding inner radius (cm)	0.4865	0.35	0.5
Spacer wire diameter (cm)	0.1	0.08	0.12
Number of pins	271	271	331
Outer core height (cm)	100	90	130
Outer-Inner heights Offset (cm)	0	0	30
Fertile plate position (% of inner height)	0	0	50
Fertile plate height (cm)	0	0	20

Table 4 – Parameters and range of variation

A space-filling design of experiment (DOE) with 5000 core designs and 8 dimensions is built. Then, the performances of these designs are evaluated with the ERANOS/MAT5DYN/GERMINAL calculation scheme.

3.3. Necessity of an optimized design of experiment

The surrogate models are built for the most important performances. The quality of each meta-model can be evaluated on an independent bunch of measures: 10% (~500 core designs) of the data basis were put aside during the kriging. The prediction or the surrogate models on this "test" set are compared to the measures. Table 5 presents the 95% (2σ) confidence interval of some meta-models.

Performance	σ95%
Extended Void effect (pcm)	110
Reactivity loss (pcm)	24
Nominal margin to melting (°C)	252
Maximal sodium T°C in ULOSSP (°C)	58

Table 5 – Performances of the surrogate models (first step)

As we can see, the main performances are quite well predicted, but the uncertainty on the prediction of the nominal margin to fusion is very high, making the surrogate model is unusable. As can be seen on fig. 5, the distribution of the margin to fuel melting in nominal conditions is unrealistic: many designs are melting in nominal conditions. It does not have any physical meaning, and it disturbs the surrogate model generation by distorting the response surface.

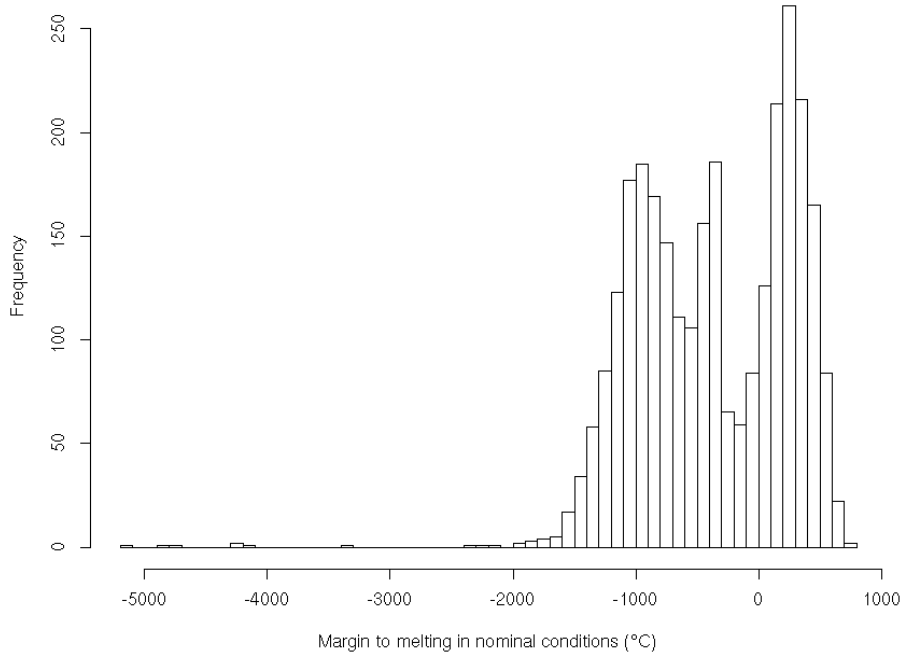

Fig. 6 - Distribution of the margins to melting in nominal conditions in the first data basis

To overcome this problem, we decided - as it was advised by other studies - to build a surrogate model for this performance, whilst excluding the designs presenting a negative margin to melting from the data basis. In that way, we used only 1100 measures for the generation of this second model, but the 95% prediction confidence is reduced to 70°C.

This model is used to generate an “optimized” design of experiment: the process is identical to the one in §3.2, but before adding a new point to the design of experiment, we evaluate its nominal margin to melting thanks to the model. Thus, the new design of experiment contains only designs with a positive (or slightly negative due to the uncertainty of the first model’s prediciton, see Fig. 7) margin to melting in nominal conditions.

 © EDF SA 2018

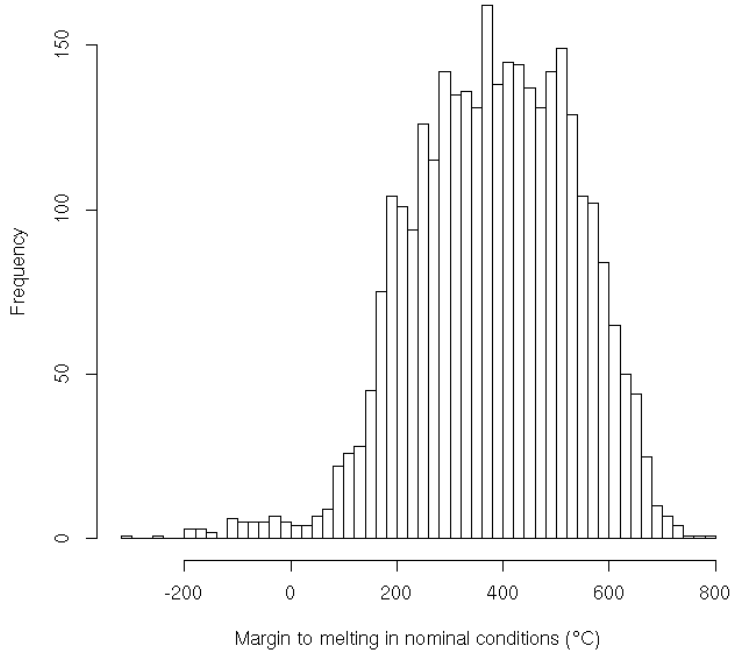

Fig. 7 Distribution of the margins to melting in nominal conditions in the second data basis

Then, the further steps of the process are repeated (calculations with the multi-physics scheme, interpolation by kriging on the new data basis). The performances of the meta-models have been improved (Table 6).

Performance	σ95%
Extended Void effect (pcm)	91
Reactivity loss (pcm)	20
Nominal margin to fusion (°C)	41
UCRW margin to melting (W/cm)	10
Maximal sodium T°C in ULOSSP (°C)	45
Breeding gain (%)	0.42

Table 6 – Performances of the surrogate models with the optimized design of experiment

 © EDF SA 2018

3.4. Analysis and choice of designs

The performances of a large amount of cores (~1,5.10^6 designs) distributed on a regular grid are evaluated with the surrogate models. Fig. 8 presents the distribution of these designs in the (Maximal sodium temperature in ULOSSP, Margin to melting during UCRW) space. First, we removed the non-viable cores, i.e. the ones that present a very low margin to fuel melting in nominal conditions.

The ULOSSP indicator is an evaluation of the maximal temperature of the sodium, with an extrapolation when it exceeds the boiling temperature. A positive margin to melting during UCRW (or δ_{UCRW}) is a guarantee of non-melting of the fuel during any UCRW transient at any time.

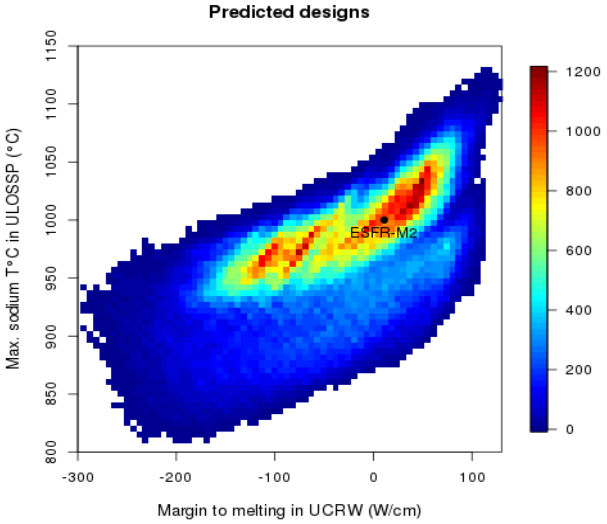

Fig. 8 – Distribution of the predicted designs in the (T_{ULOSSP}, δ_{UCRW}) space

3.4.1. Performances and parameters analysis

Then, we can analyse the distribution of the performances in this (T_{ULOSSP}, δ_{UCRW}) space and filter the most interesting designs. Fig. 9 and 10 present the total void effect (SVRE at EOEC) of the predicted designs and a zoom on the interesting area of the space, where the margin to melting during UCRW is positive. In this visualization, the color of the pixel is indexed to the mean of the performance (or parameter) of the core designs in the pixel. As we can see, we can find designs on the (T_{ULOSSP}, δ_{UCRW}) Pareto front (bottom-right frontier of the coloured surface) with a very low void effect.

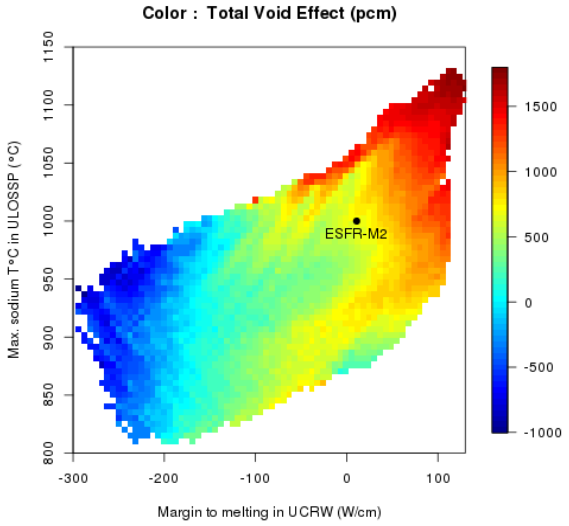

Fig. 9 - Distribution of the sodium void effect in the (T_{ULOSSP}, δ_{UCRW}) space

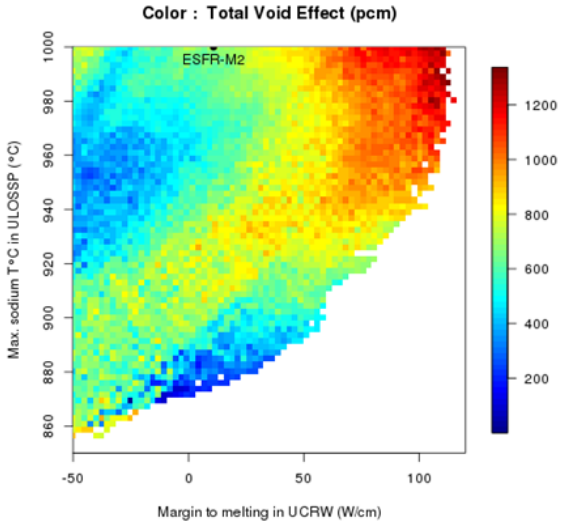

Fig. 10 - Distribution of the sodium void effect in the (T_{ULOSSP}, δ_{UCRW}) space (zoom)

Fig.11 presents the distribution of the core diameter of the predicted designs in the (SVRE, Breeding Gain) space. Beforehand, we filtered the designs that had a negative margin to melting during UCRW and a bad behaviour in case of ULOSSP. This illustration shows that it will not be possible to reduce the core diameter if we want to increase the breeding gain of the initial M2 design. The designs that have a low void effect and a near-zero breeding gain have a core diameter around 5.5m.

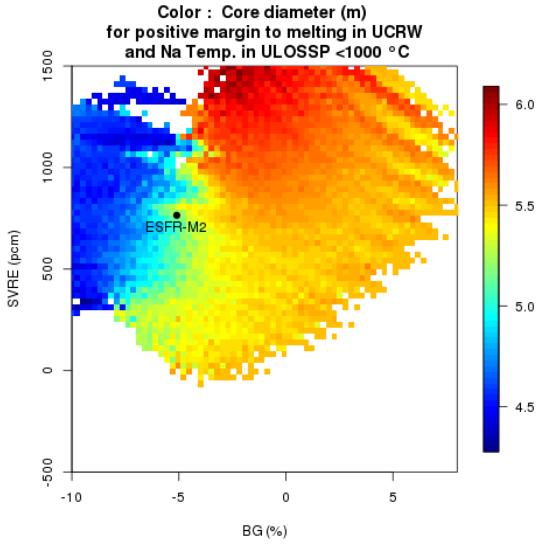

Fig. 11 - Distribution of the core diameter of the predicted designs in the (SVRE, BG) space

The following illustrations (Fig. 12 to 17) present the distribution of some parameters of the study in the (T_{ULOSSP}, δ_{UCRW}) or the (SVRE, Breeding Gain) spaces[1]. Some trends can be assessed:

- The position of the fertile plate changes along the Pareto front: a higher plate is preferable to reduce the axial power form factor and improve the UCRW behaviour. In this study, it is preferable to have a low fertile plate, in order to reduce the sodium void effect. Moreover, it is

[1] The color of the pixel is indexed to the mean of the parameter in the pixel. For example in Fig. 12, the mean of the fertile plate position in a dark blue pixel is 0%, but we can also find designs with a 10% or even 20% position at this (T_{ULOSSP}, δ_{UCRW}) point.

possible to find designs with a low fertile plate and a positive margin to melting during ULOSSP.

- Adding an inner/outer height offset between 0 and 5cm improves both ULOSSP and UCRW behaviour. Thus, it is possible to find designs with satisfying performances and no offset. This choice of parameter was not very wise.
- The outer core height should be reduced to improve the void effect and thus the ULOSSP behaviour. However, having a near-zero breeding gain implies to have a height higher than 95cm.
- The spacer wire's diameter should be reduced as low as possible: it is a win-win parameter for both ULOSSP and UCRW. However, for reasons of technical feasibility of the assembly, we decided to maintain the wire/pin diameter ratio above 0.09, as it was the case in CP-ESFR.
- The optimal value for the pellet-cladding gap is around 0.015 for these designs.

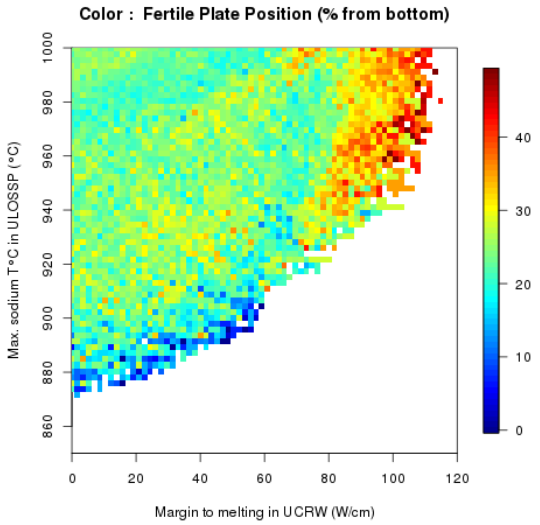

Fig. 12 - Distribution of the fertile plate position in the (T_{ULOSSP}, δ_{UCRW}) space

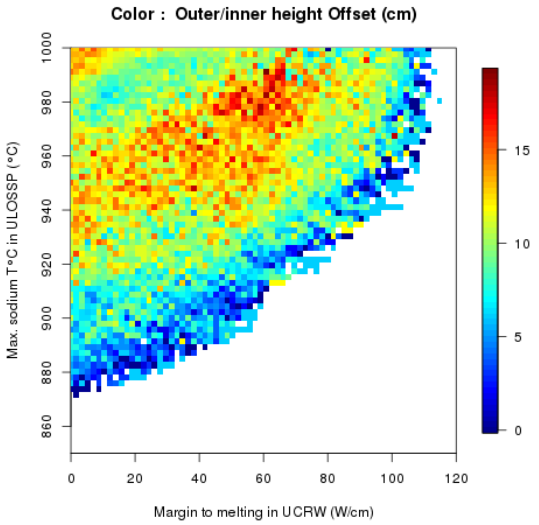

Fig. 13 - Distribution of the Outer/Inner height offset in the (T_{ULOSSP}, δ_{UCRW}) space

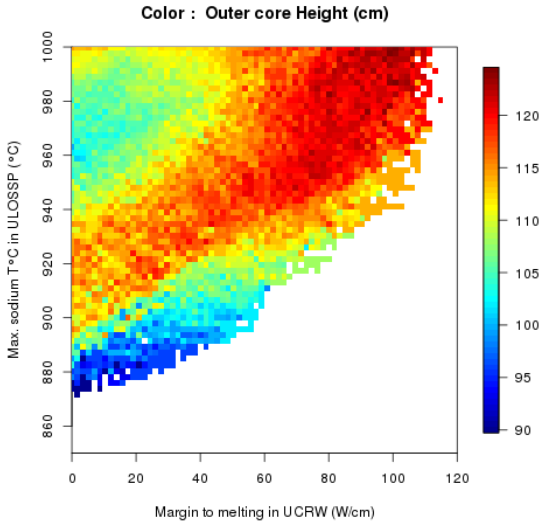

Fig. 14 - Distribution of the outer core height in the (T_{ULOSSP}, δ_{UCRW}) space

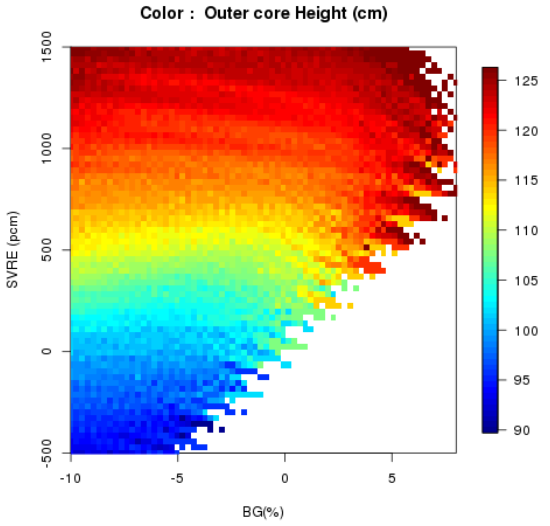

Fig. 15 - Distribution of the outer core height in the (SVRE,BG) space

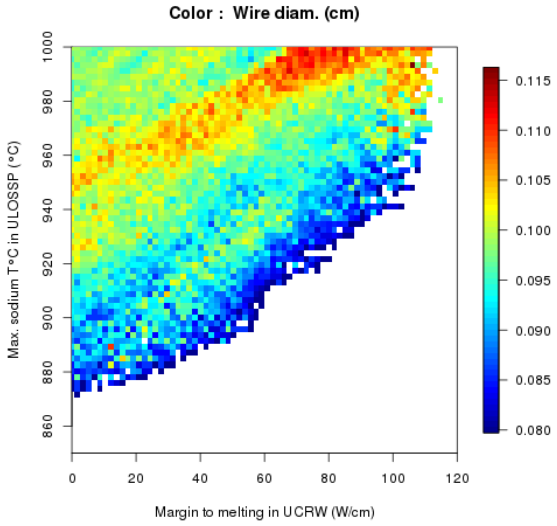

Fig. 16 - Distribution of the spacer wire diameter in the (T_{ULOSSP}, δ_{UCRW}) space

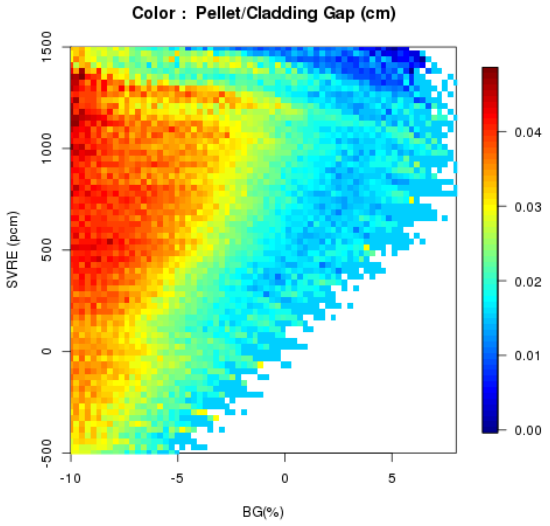

Fig. 17 - Distribution of the pellet/cladding gap width in the (SVRE, BG) space

 © EDF SA 2018

3.4.2. Design selection

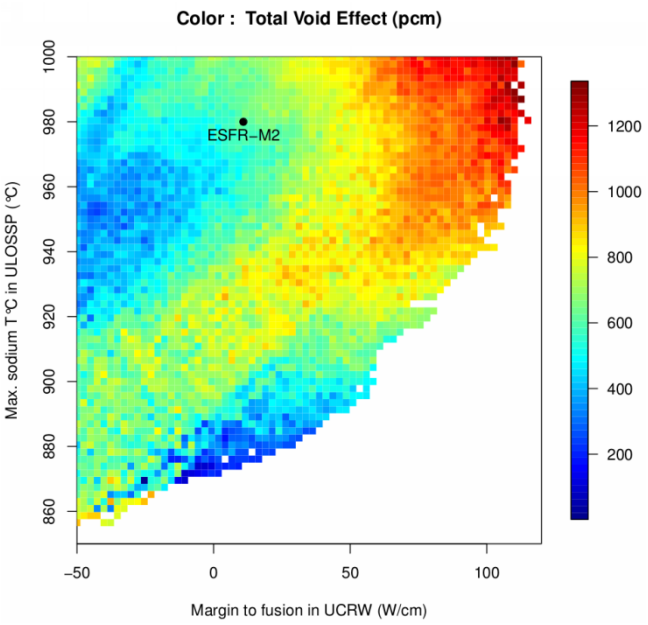

Fig. 18 - Distribution of the SVRE in the (T_{ULOSSP}, δ_{UCRW}) space

Two designs were selected after this last step of simulation, after discussion with the partners:

- The most optimized design (for the SVRE point of view) with a low fertile plate, (1)
- The most optimized design with a low fertile plate, a unique Pu enrichment, no inner/outer height offset, and a pooling of the axial elevations of the inner and outer fuel S/As to simplify the design, (2).

The characteristics and the performances of these designs are given in Table 7.

	(1)	(2)
Inner Enrich. (%vol)	17.86	**17.317**
Outer Enrich. (%vol)	16.93	**17.317**
Cycle length (EFPD)	2170	2170
Breeding Gain (BOEC)	-0.9%	-0.5%
Total SVRE (pcm) at EOEC	**20**	**153**
Estimated max. Na T°C in ULOSSP (°C)	**761**	**880**
Minimal Margin to melting in UCRW (W/cm)	**27**	**23**
KD fiss+fert (°C) 1227 --> 2300 °C	-826	-820
Outer fiss. Height (cm)	**102.5**	**95**
Inner fiss. Height (cm)	**67.5**	**75**
Outer/Inner Offset (cm)	**15**	**0**
Fertile plate height (cm)	**17.5**	**20**
Fertile plate lower bound. in the inner fissile(cm)	**0.0**	**0.0**
Fertile blanket height (cm	5	5
Inner core steel blanket (cm)	27.5	25
Pellet radius (cm)	**0.4680**	**0.4680**
Cladding inner radius (cm)	**0.4835**	**0.4835**
Clad thickness (cm)	0.05	0.05
Fuel pellet's inner hole radius (cm)	0.156	0.156
Wire diameter (cm)	0.10	0.10
Pitch (cm)	**20.985**	**20.985**

Table 7 – Performances of the selected designs

As we can see, design (1) has a lower estimated temperature in ULOSSP than expected: it does not belong to the coloured surface on fig. 18. This is the result of a bad prediction of the performance for this core, which is better than predicted by the surrogate model.

These designs present a low SVRE (below 0.5$) and a near-zero breeding gain. Their performances during a hypothetic ULOSSP or UCRW are satisfying, but they must be verified with more detailed calculation codes.

As it is important to have a simple S/A design for the ESFR-SMART project, core n°2 has been approved. Fig. 19 presents its axial layout.

 © EDF SA 2018

Inner Fuel	
Head	230
Reflector	276
Absorber	282
Reflector	18
Na Plenum	600
Plug	18
Upper gaz plenum	50
Active core	750
Fertile blanket	250
Steel blanket	250
Lower gaz plenum	913
Plug	82
Foot	370

Outer Fuel	
Head	230
Reflector	276
Absorber	282
Reflector	18
Na Plenum	600
Plug	18
Upper gaz plenum	50
Active core	950
Fertile blanket	50
Steel blanket	250
Lower gaz plenum	913
Plug	82
Foot	370

Fig. 19 – Axial layout of the selected design (n°2)

Fig. 20 and 21 present the axial power distributions in the inner and outer fuel sub-assemblies for the selected design, from position 31/30 to 42/30 (see fig.4), at beginning of each cycle of the equilibrium campaign. The effect of the reloading is noticeable in each S/A, as well as the dimming of the power at 210cm because of the control rod insertion, and its increase at 124cm in the fertile blanket due to the lower steel blanket.

 © EDF SA 2018

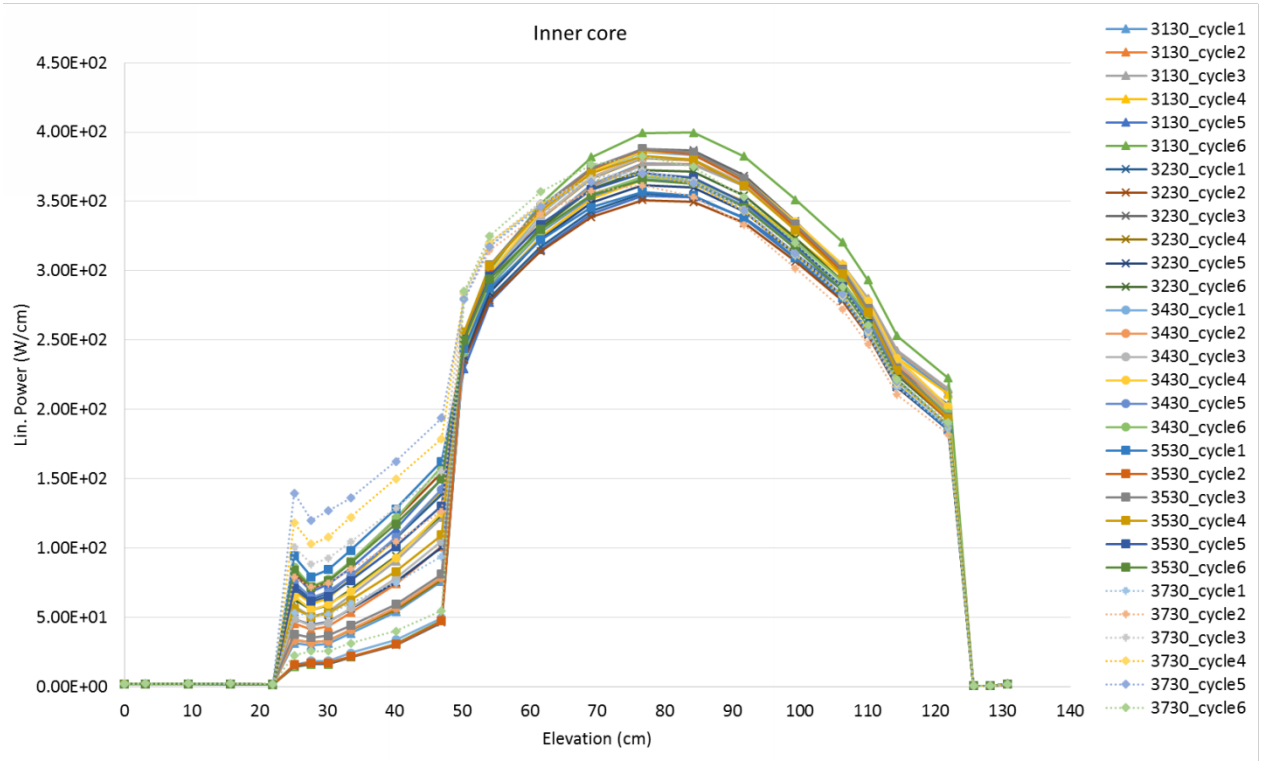

Fig. 20 – Power distribution in inner fuel S/As at positions 31/30 to 37/30 at beginning of each cycle

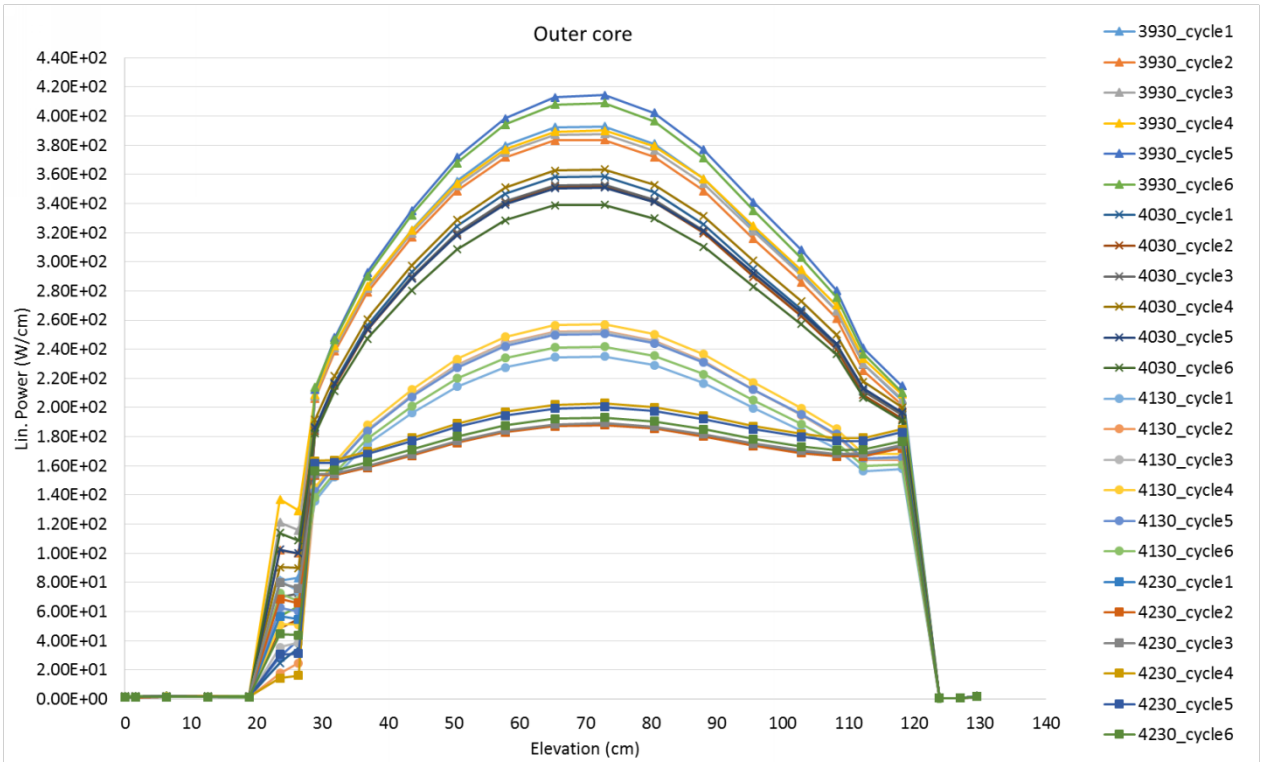

Fig. 21 - Power distribution in outer fuel S/As at positions 39/30 to 42/30 at beginning of each cycle

4. Conclusion

A large parametric space has been covered in this multi-objectives optimization study. In order to catch the global optimum in a multi-performances space, the SDDS tool has been used:

- Creation of a first design of experiment of 5000 core designs with 8 parameters : the pellet diameter, the wire diameter, the cladding diameter, the outer core height, the position and the height of the fertile plate, the outer-inner core heights offset above the fuel ;
- Simulations with SDDS's multi-physics calculation scheme (ERANOS, MAT5DYN and GERMINAL), to evaluate the performances of the previous designs
- Kriging is used to generate surrogate models for these performances and predict the behaviour of a larger panel of designs.

A two-steps procedure has been followed, as in previous studies: after a first pass of kriging, we use the surrogate models to create an optimized design of experiment, focused on the interesting area of the performances space. We simulate and krige again with this new design of experiment to build better quality meta-models and limit the prediction uncertainty.

This optimization had two main objectives, which are to improve the void effect and reach a near-zero breeding-gain, while keeping the cycle length higher than 2000 EFPD. Secondary goals were chosen, in agreement with the constraints of the ESFR-SMART project, as the limitation of the core diameter, a unique Pu content in the core, or the simplification of the axial structure of the sub-assembly by pooling the heights of the fuel or fertile parts.

A final core design was chosen and validated with the ESFR-SMART partners. It has, *inter alia*, a reduced pin radius and an increased fuel pellet hole radius, a unique Pu content, an increased fertile blanket height and a reduced fuel height. It permitted to reduce the void effect below 0.5$ at EOEC (reduction by 80% in comparison with the preliminary configuration), reach an average breeding gain of 0.5%, while simplifying the sub-assembly axial structure and therefore the further studies.

The proposition of the selected core design is a building block of the ESFR-SMART project, as it will be used to conduct number of studies: further optimization of the control rods design and the passive safety devices will be managed, as well as Monte-Carlo calculations. More detailed fuel, thermal-hydraulics, and coupled simulations will be done. The described safety measures should improve core behavior under hypothetical accident conditions that should be confirmed by analyses foreseen in ESFR-SMART.

5. Références

[1] M.C. SHEWRY H.P. WYNN, “Maximum Entropy Sampling”, *Journal of Applied Statistics*, **14**, pp. 165-170 (1987).

[2] O.ROUSTANT, D.GINSBOURGER, Y.DEVILLE, 2012. “DiceKrigin, DiceOptim: two R packages for the analysis of Computer Experiments by Kriging-based metamodeling and optimization”. Journal of statistical software, Oct.2012,Vol.51.

[3] G. RIMPAULT et al, “The ERANOS code and data system for fast reactor neutronic analyses”, *Proceedings of PHYSOR*, (2002).

[4] S. MASSARA et al, “Dynamics of critical dedicated cores for Minor Actinide Transmutation”, *Nuclear Technology*, **149**, pp. 150-174 (2005).

[5] L. ROCHE M. PELLETIER, “Modelling of the thermomechanical and physical processes in FR fuel pins using the GERMINAL code”, *Proceedings of Symposium on MOX fuel technologies for medium and long term deployment*, Vienna, (2000).

[6] F.BARJOT et al., Study of the design choice scalability to higher power level for an ASTRID-like sodium cooled fast reactor

[7] A. MARREL et al., « An efficient methodology for modelling complex computer codes with Gaussian processes », *Computational Statistics and Data Analysis,* 52:4731-4744, 2008.

[8] D. BLANCHET. L. BUIRON. 2008. “ESFR. Working Horses. Core concept definition”. FP-7-ESFR. Technical Report. CEA.